IMPERFECTION PRESSURE CORRECTIONS FOR PREDICTION OF IDEAL VAPOR-LIQUID EQUILIBRIUM RATIOS

By

JAMES RALPH RANDALL

Bachelor of Science

Oklahoma State University

Stillwater, Oklahoma

1957

Submitted to the Faculty of the Graduate School of
the Oklahoma State University,
in partial fulfillment of the requirements
for the degree of
MASTER OF SCIENCE
May 23, 1965

IMPERFECTION PRESSURE CORRECTIONS FOR PREDICTION OF IDEAL VAPOR-LIQUID EQUILIBRIUM RATIOS

Thesis Approved:

Wayne C. Edmister
Thesis Advisor

K C Chew

Dean of Graduate School

PREFACE

A generalized expression for vapor-liquid equilibrium K-values which would cover a wide range of temperatures and pressures had not been adequately developed at the time this work was undertaken. Correlations using convergence pressure had been developed, but the use of convergence pressure itself precluded generalization, so some other means was necessary. One of the most promising lines of development was thought to be through the use of the imperfection pressure correction term as applied to Raoult's Law, and to evaluate this correction term from expressions involving only generalized values. Evaluation of the imperfection pressure correction term could be made by either a density integral method, or a pressure integral method. The real problem here was to obtain the virial coefficients necessary for the evaluation of both forms before the relative merits of the two could be compared.

Appreciation is given to Professor W. C. Edmister for his guidance in pursuing the thesis subject, and Professor R. N. Maddox for the opportunity to participate in the Master's program.

The assistance of Dr. J. H. Erbar in developing some of the computer applications, and the invaluable assistance of Mr. A. N. Stuckey, Jr. are all appreciated.

My appreciation also to my parents for their encouragement and assistance, and to my wife for her understanding during the difficult times.

TABLE OF CONTENTS

LIST OF TABLES

LIST OF FIGURES

CHAPTER I

INTRODUCTION

The vapor-liquid equilibrium ratio for a component in a fluid mixture is defined as the ratio of the mole fraction of the component in the vapor phase to the mole fraction of the component in the liquid phase with which the vapor phase is in equilibrium. This is a relationship of importance to chemical engineering design, particularly in distillation and absorption calculations. The equilibrium ratio for a component in a mixture is defined as:

$$K_i = \frac{y_i}{x_i} \qquad \text{(I-1)}$$

Where: y_i is the mole fraction of the component "i" in the vapor phase, and

x_i is the mole fraction of the component "i" in the liquid phase, in equilibrium with the vapor phase, the subscript "i" will be used to indicate that a value is for a particular component

This equilibrium ratio is generally referred to as the "K-value".

The K-value is a function of pressure, temperature, volume and composition, and may be expressed as

$$K_i = K_I \frac{\gamma_i^L}{\gamma_i^V} \qquad \text{(I-2)}$$

Where: K_I is the ideal K-value for component "i", for purposes of

simplicity the "i" subscript will not be used with this term

γ_i^L is the component liquid activity coefficient

γ_i^V is the component vapor activity coefficient

The ideal K-value can be evaluated using the relationship

$$K_I = \frac{p_i^o}{\Theta_i P} \qquad \text{(I-3)}$$

Where: p_i^o is the component vapor pressure

P is the system pressure

Θ_i is the component imperfection pressure correction term, which corrects for the component's deviation from Raoult's Law

Stuckey (4) evaluated the imperfection pressure correction term using the Berlin form of the equation for this term. Stuckey used Pitzer's equation (3) for the second virial coefficient, and developed an equation for the third virial coefficient, which was used in the Berlin form of the imperfection pressure correction equation. The third virial coefficient equation was developed using convergence pressure, and through it a relationship was developed which allowed reliable K-value evaluation up to a reduced pressure of 6.29. One intention of this thesis originally was to continue the work done by Stuckey and to extend the pressure range of the imperfection pressure correction term using convergence pressure to obtain other virial coefficient equations. The convergence pressure concept was discarded, however, after it was decided that it would be more advantageous to have a strictly general expression.

A generalized evaluation of the imperfection pressure correction term requires the use of generalized virial coefficients. Pitzer's

equation could possibly be used for the second virial, and equations for additional virial coefficients as functions of reduced temperature and acentric factor (3) could be obtained from correlations of generalized data. Compressibility data as a function of reduced temperature, reduced pressure and acentric factor are available (3). The compressibility factor can be expressed as a virial equation in either a pressure or density series. This would allow the virial coefficients to be obtained from a power series correlation of compressibility with either pressure or density. The imperfection pressure correction term can be evaluated by integrating to either pressure or density, using the appropriate virial coefficients. This would allow a comparison of ideal K-values calculated by the two different methods.

The ideal K-value can also be expressed[1] in the form (4)

$$K_I = K_I^o (K_I')^{\omega} \qquad \text{(I-4)}$$

Where: K_I^o is the ideal K-value the component would have at the system temperature and pressure if it were a simple fluid

K_I' is the correction for the deviation of the behavior of the component from that of a simple fluid, also at the temperature and pressure of the system

ω is the acentric factor of the component (3)

K_I^o and K_I' are functions of reduced pressure and reduced temperature, only. The acentric factor is a value unique to the particular component being considered, and for a simple fluid component it is zero. The relationship shown in Equation (I-4) is a convenient one, and it gives

---

[1]Later work prior to publication of this thesis has disproved the validity of this mathematical model.

a continuity of form with other Pitzer-type (3) thermodynamic relationships. Taking logarithms of both sides of Equation (I-4)

$$\ln K_I = \ln K_I^o + \omega \ln K_I' \qquad \text{(I-5)}$$

which can be rearranged to give the expression

$$\ln K_I' = (\ln K_I - \ln K_I^o)/\omega \qquad \text{(I-6)}$$

K_I' at a certain pressure and temperature can be determined from Equation (I-6) if K_I and K_I^o are first evaluated from Equation (I-3) using an acentric factor of ω for the former and an acentric factor of 0 for the latter.

The ratio of the activity coefficients shown in Equation (I-2) can be obtained by dividing the experimental K-value by the ideal K-value. The liquid activity coefficient can be evaluated by the Scatchard-Hildebrand (7) equation, allowing the vapor activity coefficient to be determined from the activity coefficient ratio.

Purpose of This Work

The purpose of this work is to obtain generalized virial coefficients for use in evaluating the Berlin and Leiden forms of the equation for the imperfection pressure correction term: to make a comparison of the ideal K-values obtained using each form, then to use the improved ideal K-value correlation to obtain vapor phase activity coefficients from fluid mixture experimental data.

CHAPTER II

IMPERFECTION PRESSURE CORRECTION TERM EQUATIONS AND VIRIAL COEFFICIENT RELATIONSHIPS

The liquid and vapor phases of a fluid mixture are in equilibrium if their temperatures and pressures are equal, and if

$$\bar{f}_i^L = \bar{f}_i^V \tag{II-1}$$

Where: $\bar{f}_i^L$ is the liquid phase fugacity of component "i" in the fluid mixture at the system temperature and pressure

$\bar{f}_i^V$ is the vapor phase fugacity of component "i" in the fluid mixture at the system temperature and pressure

Combining Equations (I-1) and (II-1) will give

$$K_i = \frac{\bar{f}_i^L / x_i}{\bar{f}_i^V / y_i} \tag{II-2}$$

Equation (II-2) can be written in an equivalent form

$$K_i = \left(\frac{\bar{f}_i^L / f_i^L x_i}{\bar{f}_i^V / f_i^V y_i} \right) \left(\frac{f_i^L / p_i^o}{\bar{f}_i^V / P} \right) \left(\frac{p_i^o}{P} \right) \tag{II-3}$$

Where, by definition:

$$\gamma_i^L = \frac{\bar{f}_i^L}{f_i^L x_i} \tag{II-4a}$$

$$\gamma_i^V = \frac{\bar{f}_i^V}{f_i^V y_i} \qquad \text{(II-4b)}$$

$$\theta_i = \frac{f_i^V / P}{f_i^L / p_i^o} \qquad \text{(II-4c)}$$

$$K_{Raoult} = \frac{p_i^o}{P} \qquad \text{(II-4d)}$$

and

$$K_I = \frac{K_{Raoult}}{\theta_i} \qquad \text{(II-5)}$$

Equation (II-3) can now be written

$$K_i = \left(\frac{\gamma_i^L}{\gamma_i^V} \right) K_I \qquad \text{(II-6)}$$

Taking logarithms of Equation (II-4c) at constant system pressure gives

$$\ln \theta_i = \ln \left(\frac{f_i^V}{P} \right)_P - \ln \left(\frac{f_i^L}{p_i^o} \right)_P \qquad \text{(II-7)}$$

The remainder of this chapter will be devoted to the evaluation of Equation (II-7).

Free energy is defined as

$$F = H - TS \qquad \text{(II-8)}$$

Where:

F is the free energy of the system under consideration

H is the enthalpy of the system

S is the entropy of the system

T is the temperature of the system

Differentiating Equation (II-8) gives

$$dF = dH - TdS - SdT \qquad \text{(II-9)}$$

Enthalpy is defined as

$$H = E + PV \qquad \text{(II-10)}$$

Where:

E is the energy of the system

P is the pressure of the system

V is the volume of the system

Differentiating Equation (II-10) gives

$$dH = dE + PdV + VdP \qquad \text{(II-11)}$$

Combining Equations (II-9) and (II-11) gives

$$dF = -SdT + VdP \qquad \text{(II-12)}$$

For an isothermal process Equation (II-12) becomes

$$dF = VdP \qquad \text{(II-13)}$$

Integrating between the limits of the component vapor pressure and the system pressure gives

$$F_P - F_{p_i^o} = \int_{p_i^o}^{P} V dP \qquad \text{(II-14)}$$

Where:

F_P is the free energy of the system at the system temperature and pressure

$F_{p_i^o}$ is the free energy of the system at the system temperature and the component vapor pressure

For an ideal gas

$$V = \frac{RT}{P} \qquad \text{(II-15)}$$

Combining Equations (II-14) and (II-15) gives

$$F_P - F_{p_i^o} = \int_{p_i^o}^{P} \frac{RT}{P} dP \qquad \text{(II-16)}$$

At constant system temperature Equation (II-16) becomes

$$F_P - F_{p_i^o} = RT \ln \frac{P}{p_i^o} \qquad \text{(II-17)}$$

For the case of a real gas, pressures would be replaced by fugacities and Equation (II-17) would become

$$F_P - F_{p_i^o} = RT \ln \frac{f_P}{f_{p_i^o}} \qquad \text{(II-18)}$$

Where:

f_P is the fugacity of the system at the system temperature and system pressure

$f_{p_i^o}$ is the fugacity of the system at the system temperature and the vapor pressure of component "i"

Combining Equations (II-14) and (II-18) gives

$$RT \ln \frac{f_P}{f_{p_i^o}} = \int_{p_i^o}^{P} V dP \qquad \text{(II-19)}$$

Equation (II-19) is an expression for a fluid mixture system, the vapor and liquid phases of this system will have the following corresponding expressions for component "i"

$$RT \ln \frac{\left(f_i^V\right)_P}{\left(f_i^V\right)_{p_i^o}} = \int_{p_i^o}^{P} V_i \, dP \qquad \text{(II-20)}$$

and

$$RT \ln \frac{\left(f_i^L\right)_P}{\left(f_i^L\right)_{p_i^o}} = \int_{p_i^o}^{P} V_i^L \, dP \qquad \text{(II-21)}$$

Where:

V_i is the component vapor phase molar volume

V_i^L is the component liquid phase molar volume

The difference between the volumes of a real and an ideal gas is known as the residual gas volume. Symbolically this is

$$\alpha_i = \frac{RT}{P} - V_i \qquad \text{(II-22)}$$

Combining Equations (II-20) and (II-22) gives

$$RT \ln \frac{\left(f_i^V\right)_P}{\left(f_i^V\right)_{p_i^o}} = RT \ln \frac{P}{p_i^o} - \int_{p_i^o}^{P} \alpha_i \, dP \qquad \text{(II-23)}$$

Rearranging Equation (II-23) gives

$$RT \left[\ln \left(\frac{f_i^V}{P} \right)_P + \ln \left(\frac{f_i^V}{p_i^o} \right)_{p_i^o} \right] = - \int_{p_i^o}^{P} \alpha_i \, dP \qquad \text{(II-24)}$$

By allowing the vapor pressure to approach zero, the second left hand side term disappears and Equation (II-24) becomes

$$RT \ln \left(\frac{f_i^V}{P} \right)_P = - \int_0^P \alpha_i \, dP \qquad \text{(II-25)}$$

Combining Equations (II-22) and (II-25) gives

$$\ln \left(\frac{f_i^V}{P} \right)_P = \frac{1}{RT} \int_0^P \left(V_i - \frac{RT}{P} \right) dP \qquad \text{(II-26)}$$

which is seen to be the first term on the right hand side of Equation (II-7), the imperfection pressure correction equation.

At equilibrium, the fugacities of pure component "i" in the liquid and vapor phases at the system temperature and the vapor pressure are equal, or

$$\left(f_i^L \right)_{p_i^o} = \left(f_i^V \right)_{p_i^o} \qquad \text{(II-27)}$$

Combining Equations (II-21) and (II-27) gives

$$RT \ln \frac{\left(f_i^L \right)_P}{\left(f_i^V \right)_{p_i^o}} = \int_{p_i^o}^P V_i^L \, dP \qquad \text{(II-28)}$$

Since a pure component is being considered, the vapor pressure is the same as the system pressure, or

$$p_i^o = P$$

Dividing the numerator of the left hand term of Equation (II-28) by p_i^o, and the denominator by P will not alter the term's value. The equation will become

$$\ln\left(\frac{f_i^L}{p_i^o}\right)_P = \ln\left(\frac{f_i^V}{P}\right)_{p_i^o} + \frac{1}{RT}\int_{p_i^o}^{P} V_i^L \, dP \qquad \text{(II-29)}$$

which is seen to be the second term on the right hand side of Equation (II-7). The last term in Equation (II-29) is known as the "Poynting Effect", which corrects the liquid fugacity from the vapor pressure to the system pressure. By analogy to Equation (II-26) the first right hand side term of Equation (II-29) may be written

$$\ln\left(\frac{f_i^V}{P}\right)_{p_i^o} = \frac{1}{RT}\int_{0}^{p_i^o}\left(V_i - \frac{RT}{P}\right) dP \qquad \text{(II-30)}$$

Upon combining Equations (II-7), (II-26), (II-29) and (II-30) there results

$$\ln \Theta_i = \frac{1}{RT}\int_{p_i^o}^{P}\left(V_i - \frac{1}{RT}\right) dP - \frac{1}{RT}\int_{p_i^o}^{P} V_i^L \, dP \qquad \text{(II-31)}$$

The Berlin solution (so called because it is based on the Berlin form of the virial equation of state) of Equation (II-31) can be found by utilizing the pressure series equation of state for a component

$$PV_i = RT + B_i'P + C_i'P^2 + \cdots \qquad \text{(II-32)}$$

Where:

R is the universal gas constant

B_i' is the component second Berlin virial coefficient

C_i' is the component third Berlin virial coefficient

From Equation (II-32) the component molar vapor volume can be expressed

$$V_i = \frac{RT}{P} + B_i' + C_i'P + \cdots \qquad \text{(II-33)}$$

Combining Equations (II-31) and (II-33) will give a differential equation. If V_i^L is assumed constant between the limits p_i^o and P, the equation can be integrated to give

$$\ln \Theta_i = \frac{1}{RT}\left[\left(B_i' - V_i^L\right)\left(P - p_i^o\right) + \frac{C_i'}{2}\left(P^2 - p_i^{o\,2}\right) + \cdots\right] \qquad \text{(II-34)}$$

Dividing Equation (II-32) by RT will give

$$Z_i = 1 + \frac{B_i'P}{RT} + \frac{C_i'P^2}{RT} + \cdots \qquad \text{(II-35)}$$

Using the following definitions:

$$B_i'' = \frac{1}{T_r}\left(\frac{B_i'P_c}{RT_c}\right) \qquad \text{(II-36a)}$$

$$C_i'' = \frac{1}{T_r}\left(\frac{C_i' P_c^{\,2}}{RT_c}\right) \qquad \text{(II-36b)}$$

Where:

B_i'' is the component generalized second Berlin virial coefficient

C_i'' is the component generalized third Berlin virial coefficient

T_r is the reduced system temperature

T_c is the component critical temperature

P_r is the reduced system pressure

P_c is the component critical pressure

and, in addition

p_r^o is the component reduced vapor pressure

The relationships between the above mentioned reduced and critical properties are:

$$P_r = \frac{P}{P_c}$$

$$p_r^o = \frac{p_i^o}{P_c}$$

$$T_r = \frac{T}{T_c}$$

Equation (II-35) can now be written

$$Z_i = 1 + B_i'' P_r + C_i'' P_r^{\,2} + \cdots \qquad \text{(II-37)}$$

and Equation (II-34) can now be written

$$\ln \theta_i = \left(B_i'' - \frac{1}{T_r}\frac{V_i^L P_c}{RT_c}\right)\left(P_r - p_r^o\right) + \frac{C_i''}{2}\left(P_r^2 - p_r^{o2}\right) + \cdots \quad \text{(II-38)}$$

where:

$\frac{V_i^L P_c}{RT_c}$ is the component reduced liquid phase molar volume, as defined in Appendix B

Equation (II-38) is the generalized Berlin form of the imperfection pressure correction term equation which will be used in the calculations in Chapter IV. Equation (II-38) will be referred to as the "pressure integral" method in the following chapters. The generalized Berlin virial coefficients take into consideration the vapor volume only.

Another solution to Equation (II-31) can be obtained, the Leiden Solution, so called because it is based on the Leiden form of the virial equation of state. The first term on the right hand side of Equation (II-31) can be evaluated in the following manner:

$$\frac{1}{RT}\int_{p_i^o}^{P}\left(V_i - \frac{RT}{P}\right)dP = \frac{1}{RT}\int_{p_i^o}^{P} V_i\, dP - \int_{p_i^o}^{P} d\ln P \quad \text{(II-39)}$$

$$\frac{1}{RT}\int_{p_i^o}^{P} V_i \, dP = \frac{1}{RT}\left(PV_i\right)_{p_i^o}^{P} - \int_{V_{i(p_i^o)}}^{V_{i(P)}} \frac{P}{RT} \, dV_i \qquad \text{(II-40)}$$

$$\frac{1}{RT}\left(PV_i\right)_{p_i^o}^{P} = \left(Z_i\right)_{p_i^o}^{P} \qquad \text{(II-41)}$$

$$\int_{V_{i(p_i^o)}}^{V_{i(P)}} \frac{P}{RT} \, dV_i = \int_{V_{i(p_i^o)}}^{V_{i(P)}} \frac{Z_i}{V_i} \, dV_i \qquad \text{(II-42)}$$

The density series equation of state is

$$Z_i = 1 + \frac{B_i}{V_i} + \frac{C_i}{V_i^2} + \cdots \qquad \text{(II-43)}$$

Where:

Z_i is the component vapor phase compressibility factor

B_i is the component second Leiden virial coefficient

C_i is the component third Leiden virial coefficient

Combining Equations (II-42) and (II-43) gives

$$\int_{V_{i(p_i^o)}}^{V_{i(P)}} \frac{P}{RT}\, dV_i = \int_{V_{i(p_i^o)}}^{V_{i(P)}} \left(\frac{1}{V_i} + \frac{B_i}{V_i^2} + \frac{C_i}{V_i^3} + \cdots \right) dV_i \qquad \text{(II-44)}$$

and, upon integration

$$\int_{V_{i(p_i^o)}}^{V_{i(P)}} \frac{P}{RT}\, dV_i = \left(\ln V_i - \frac{B_i}{V_i} - \frac{C_i}{2V_i^2} + \cdots \right)_{V_{i(p_i^o)}}^{V_{i(P)}} \qquad \text{(II-45)}$$

Combining Equations (II-40), (II-41) and (II-45) gives

$$\frac{1}{RT} \int_{p_i^o}^{P} V_i\, dP = \left(Z_i - \ln V_i + \frac{B_i}{V_i} + \frac{C_i}{2V_i^2} + \cdots \right)_{V_{i(p_i^o)}}^{V_i} \qquad \text{(II-46)}$$

Utilizing the relationship

$$-\int_{p_i^o}^{P} d \ln P = \left(\ln P \right)_{p_i^o}^{P} \qquad \text{(II-47)}$$

along with Equations (II-46) and (II-39) gives

$$\frac{1}{RT}\int_{p_i^o}^{P}\left(V_i - \frac{RT}{P}\right)dP = \left[Z_i - \ln PV_i + \frac{B_i}{V_i} + \frac{C_i}{2V_i^2} + \cdots\right]_{p_i^o}^{P} \qquad \text{(II-48)}$$

When the vapor pressure is zero, the following occurs:

$$Z_{i_{(p_i^o)}} = 1 \qquad \text{(II-49a)}$$

$$\ln p_i^o V_{i_{(p_i^o)}} = \ln RT \qquad \text{(II-49b)}$$

By combining Equations (II-43) and (II-48), and utilizing Equations (II-49a) and (II-49b), there can be obtained (allowing the vapor pressure to go to zero)

$$\frac{1}{RT}\int_{0}^{P}\left(V_i - \frac{RT}{P}\right)dP = \frac{2B_i}{V_{i_{(P)}}} + \frac{3C_i}{2V_{i_{(P)}}^2} + \cdots - \ln Z_{i_{(P)}} \qquad \text{(II-50)}$$

An equation similar to Equation (II-50) can be obtained between the limits of p_i^o and 0, which can be combined with Equation (II-50) to give

$$\frac{1}{RT}\int_{p_i^o}^{P}\left(V_i - \frac{RT}{P}\right)dP = \frac{2B_i}{V_{i_{(P)}} - V_{i_{(p_i^o)}}} + \frac{3C_i}{2\left(V_{i_{(P)}}^2 - V_{i_{(p_i^o)}}^2\right)}$$

$$+ \cdots - \ln \frac{Z_{i_{(P)}}}{Z_{i_{(p_i^o)}}} \qquad \text{(II-51)}$$

The second term in Equation (II-31) can be obtained by direct integration

$$\frac{1}{RT}\int_{p_i^o}^{P} V_i^L\, dP = \frac{V_i^L}{RT}\left(P - p_i^o\right) \qquad \text{(II-52)}$$

Equation (II-52) can be expressed in an equivalent form as

$$\frac{1}{RT}\int_{p_i^o}^{P} V_i^L\, dP = \frac{1}{T_r}\left(\frac{V_i^L P_c}{RT_c}\right)\left(P_r - p_r^o\right) \qquad \text{(II-53)}$$

Where the reduced liquid volume term is evaluated in Appendix B,

as mentioned before.

Combining Equations (II-31), (II-51) and (II-53) will give

$$\ln \theta_i = 2B_i \left(\frac{1}{V_{i(P)}} - \frac{1}{V_{i(p_i^o)}} \right) + \frac{3}{2} C_i \left(\frac{1}{V_{i(P)}^2} - \frac{1}{V_{i(p_i^o)}^2} \right)$$

$$+ \ldots - \frac{1}{T_r} \left(\frac{V_i^L P_c}{RT_c} \right) \left(P_r - p_r^o \right) \qquad \text{(II-54)}$$

Equation (II-54) is a Leiden form of the equation for the imperfection pressure correction term. This equation may be generalized by making use of the relationships

$$\frac{B_i}{V_i} = \left(\frac{B_i P_c}{RT_c} \right) \left(\frac{P_r}{Z_i T_r} \right) \qquad \text{(II-55a)}$$

$$\frac{C_i}{V_i^2} = \left(\frac{C_i P_c^2}{R^2 T_c^2} \right) \left(\frac{P_r}{Z_i T_r} \right)^2 \qquad \text{(II-55b)}$$

Equation (II-43) may now be written

$$Z_i = 1 + \left(\frac{B_i P_c}{RT_c} \right) \left(\frac{P_r}{Z_i T_r} \right) + \left(\frac{C_i P_c^2}{R^2 T_c^2} \right) \left(\frac{P_r}{Z_i T_r} \right)^2 + \ldots \qquad \text{(II-56)}$$

The following relationships will be defined:

$$b_i = \frac{B_i P_c}{RT_c} \qquad \text{(II-57a)}$$

$$c_i = \frac{C_i P_c^2}{R^2 T_c^2} \qquad \text{(II-57b)}$$

$$\rho_r = \frac{P_r}{Z_i V T_r} \qquad \text{(II-57c)}$$

Where:

b_i is the component second generalized Leiden virial coefficient

c_i is the component third generalized Leiden virial coefficient

ρ_r is the component reduced density

Equation (II-56) may now be written in a generalized form

$$Z_i = 1 + b_i \rho_r + c_i \rho_r^2 + \cdots \qquad \text{(II-58)}$$

Equation (II-54) can also be written in a generalized form

$$\ln \Theta_i = 2b_i \left(\rho_{r_{(P)}} - \rho_{r_{(p_i^o)}}\right) + \frac{3}{2} c_i \left(\rho^2_{r_{(P)}} - \rho^2_{r_{(p_i^o)}}\right)$$

$$+ \cdots - \frac{1}{T_r} \frac{V_i^L P_c}{RT_c} \left(P_r - p_r^o\right) \qquad \text{(II-59)}$$

Equation (II-59) is the generalized Leiden form of the imperfection pressure correction term, and will be used in the calculations in Chapter IV. The Leiden generalized virial coefficients take into consideration only the vapor phase volume, as did the Berlin coefficients. In the following chapters Equation (II-59) will be referred to as the "density integral" method.

CHAPTER III

EVALUATION OF VIRIAL COEFFICIENTS

The generalized second Berlin virial coefficient, B_i'', can be evaluated by combining Equation (II-35a), $B_i'' = 1/T_r\ (B_i' P_c/RT_c)$, with an equation developed by Pitzer (3)

$$\frac{B_i' P_c}{RT_c} = (0.1145 + 0.073\omega) - (0.330 - 0.46\omega)T_r - (0.1385 + 0.50\omega)T_r^2 - (0.01212 + 0.097\omega)T_r^3 - 0.0073\omega/T_r^8 \qquad \text{(III-1)}$$

The generalized third Berlin virial coefficient, C_i'', can be evaluated using Equation (II-37), $Z_i = 1 + B_i'' P_r + C_i'' P_r^2 + \cdots$ Equation (II-37) can be rearranged into the form

$$\frac{Z_i - 1 - B_i'' P_r}{P_r^2} = C_i'' + D_i'' P_r + \cdots \qquad \text{(III-2)}$$

from which C_i'' can be determined as the intercept of the plot $(Z_i - 1 - B_i'' P_r)/P_r^2$ vs P_r. The slope of the curve at the intercept will be D_i''. A method similar to Equation (III-2) can be extended to obtain the higher generalized Berlin virial coefficients. In Equation (III-2), B_i'' can be calculated as mentioned above. The value of Z_i can be obtained using Pitzer's (3) generalized compressibility factor data. This data is listed as a function of T_r and P_r, and is in two parts: (1) The simple fluid compressibility factor, Z_i^o; and (2) The deviation of the compressi-

bility factor from the simple fluid, $Z_i^!$. The component compressibility factor is calculated from this data using the relationship (3)

$$Z_i = Z_i^o + \omega Z_i^! \qquad \text{(III-3)}$$

The generalized second Leiden virial coefficient can be obtained using the relationship

$$b_i = B_i^{"} \qquad \text{(III-4)}$$

In Equation (III-4), $B_i^{"}$ can be calculated as previously mentioned, and $V_i^L P_c/RT_c$ is the component reduced liquid phase molar volume introduced in Equation (II-37). This term can be evaluated by means of Equation (B-1) in Appendix B.

The generalized third Leiden virial coefficient can be obtained using the relationship

$$c_i = C_i^{"} T_r + B_i^{"2} \qquad \text{(III-5)}$$

Equations (III-4) and (III-5) allow generalized Leiden virial coefficients to be evaluated from generalized Berlin virial coefficients. However, the generalized Leiden virial coefficients can be evaluated independently. The relationship between the second Leiden virial coefficient and the second Berlin virial coefficient is

$$B_i = B_i^! \qquad \text{(III-6)}$$

Substituting B_i for $B_i^!$ in Equation (III-1) and combining with Equation (II-57a), $b_i = (B_i P_c/RT_c)$, will provide a means for calculating b_i. In other words b_i is equal to the right hand side of Equation (III-1). The generalized third Leiden virial coefficient can be evaluated using

Equation (II-57), $Z_i = 1 + b_i\rho_r + c_i\rho_r + \cdots$. Equation (II-57) can be rearranged into the form

$$\frac{Z_i - 1 - b_i\rho_r}{\rho_r^2} = c_i + d_i\rho_r + \cdots \qquad \text{(III-7)}$$

from which c_i can be evaluated as the intercept of the plot $(Z_i - 1 - b_i\rho_r)/\rho_r^2$ vs ρ_r. The slope of the curve at the intercept will be d_i. The method used to obtain Equation (III-7) can be extended to obtain the higher generalized Leiden virial coefficients.

The generalized second and third Berlin virial coefficients can be obtained from the generalized Leiden virial coefficients using

$$B_i'' = b_i \qquad \text{(III-8)}$$

and

$$C_i'' = \frac{(c_i - b_i^2)}{T_r} \qquad \text{(III-9)}$$

The preceding discussion has covered the methods which can be used to obtain virial coefficients. The remainder of this chapter will be devoted to a discussion of actual results obtained when these methods were applied.

Pressure Series Evaluation Via Curve Fitting

The first attempt to obtain virial coefficients were made using the previously mentioned Pitzer's compressibility data, Pitzer's equation for B_i'', and the relationship given in Equation (III-2). The conditions chosen were for an acentric factor of 0 and a reduced temperature of 1.0. Values of $(Z_i - 1 - B_i''P_r)/P_r^2$ were calculated for various P_r's and

plotted as shown in Figure 1. The intercept of this plot at zero pressure should be C_i'', and the slope of the curve at the intercept should be D_i''. The points shown in Figure 1 were too irregular to allow a reliable determination of C_i'' and D_i''.

In order to check the feasibility of determining D_i'' from an intercept, values of $(Z_i - 1 - B_i''P_r - C_i''P_r^2)/P_r^3$ were calculated for various P_r's and plotted as shown in Figure 2. Comparing Figures 1 and 2 shows the situation now to be even worse than before, and there is no chance of getting reliable determination of D_i'' as a curve intercept. The greater irregularity of Figure 2 is probably due to the fact that the value of C_i'' used in the calculations was estimated from the intercept of Figure 1.

So far, no curve fit of the data had been attempted. The points obtained using a reduced pressure basis were of an irregular nature, and not likely to permit a good curve fit determination of the virial coefficients. At this point, it was noted that the density series equation of state would be somewhat more convenient with which to work. This, plus the hope that points obtained using generalized density would minimize the irregularity previously observed, led to the next step.

Density Series Evaluation Via Curve Fitting

The next phase of the investigation involved using the density series equation of state, as given in Equation (II-57). The rearrangement of this equation given in Equation (III-7) allows a plot to be made of $(Z_i - 1 - b_i \rho_r)/\rho_r^2$ vs ρ_r, which will give c_i as the intercept and d_i as the slope at the intercept. Values of this were calculated for various reduced densities, at an acentric factor of 0 and a reduced temperature of 1.0. These values are tabulated in Table 1, and plotted

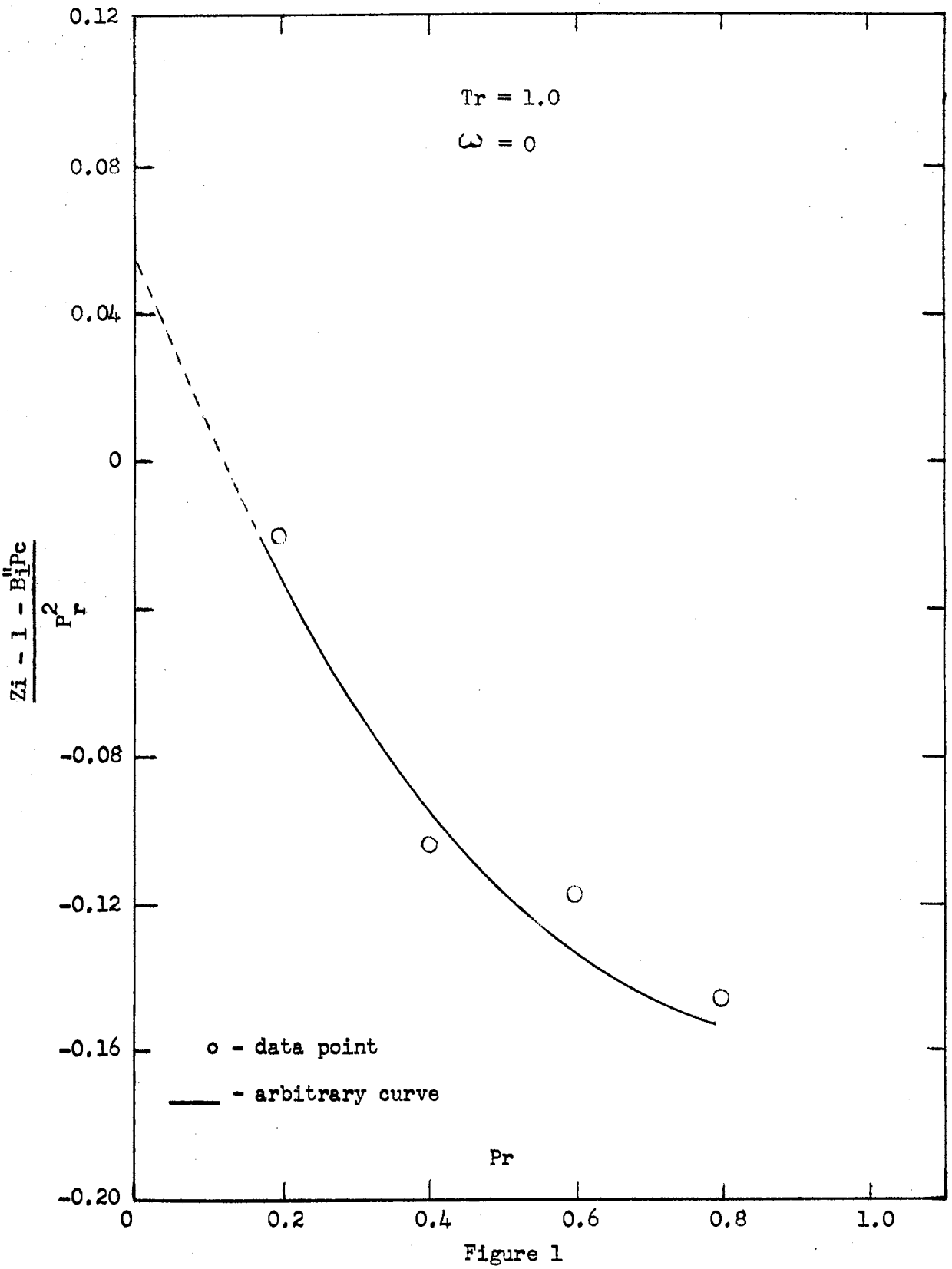

Figure 1

Determination of C_1'' Using a Reduced Pressure Basis

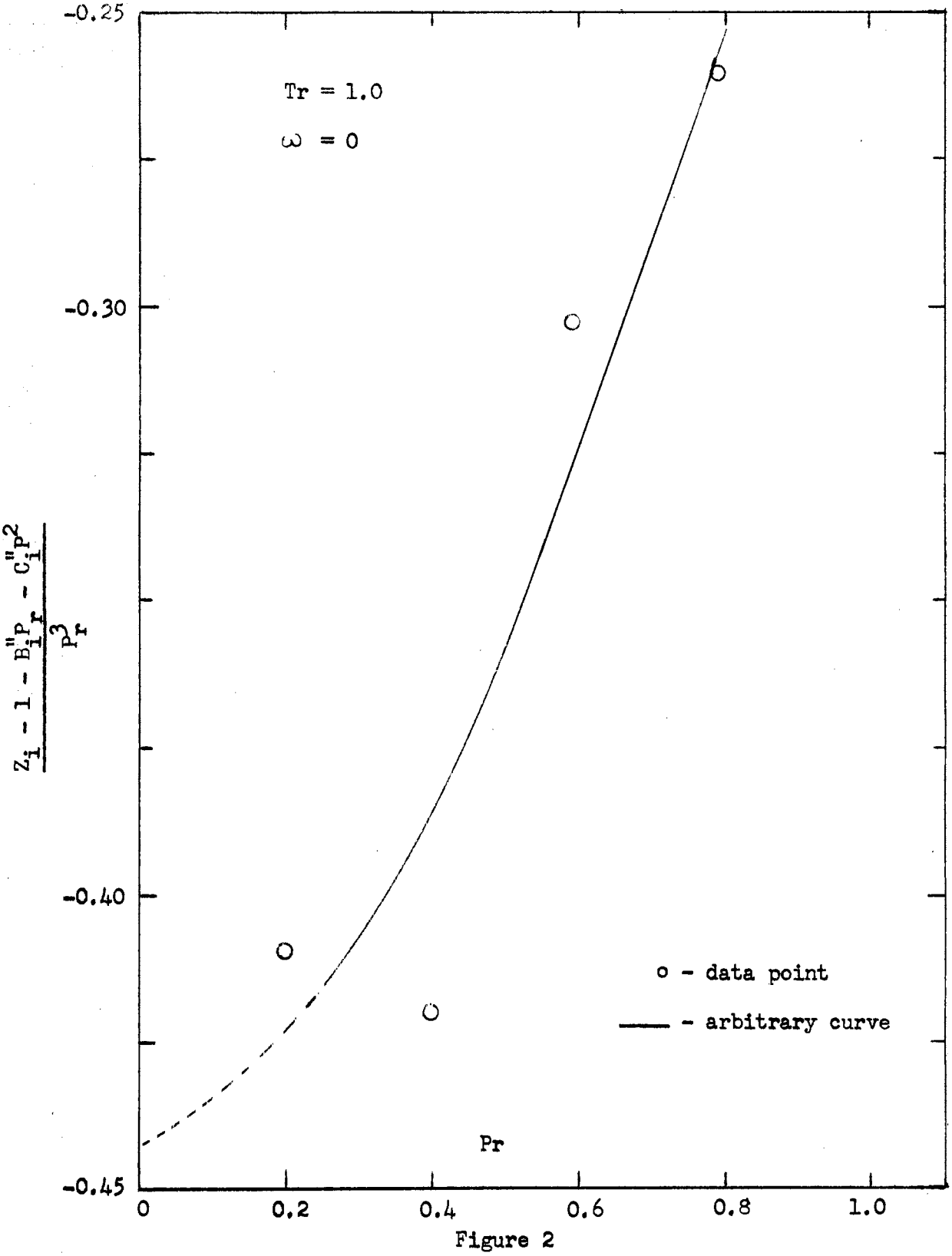

Figure 2

Determination of D_i'' Using a Reduced Pressure Basis

Table 1

Data for c_i Determination by Least Squares Curve Fit.

$T_r = 1.0, \omega = 0$

ρ_r	$\frac{Z_i - 1 - b_i \rho_r}{\rho_r^2}$
0.2146	0.08957
0.4711	0.03312
0.7937	0.03611
1.2539	0.03780
3.4364	0.03777
5.1948	0.03620
5.6000	0.03610
5.7554	0.03660
5.9211	0.03691
6.0790	0.03713
6.1798	0.03752
6.2992	0.03776
6.3882	0.03808
6.4665	0.03842
6.5502	0.03868
6.1157	0.03903
6.6797	0.03931
6.7416	0.03960
6.8223	0.03974
6.8729	0.04005
7.0093	0.04066
7.1225	0.04131
7.3260	0.04251
7.5107	0.04354
7.6336	0.04485
7.7187	0.04633

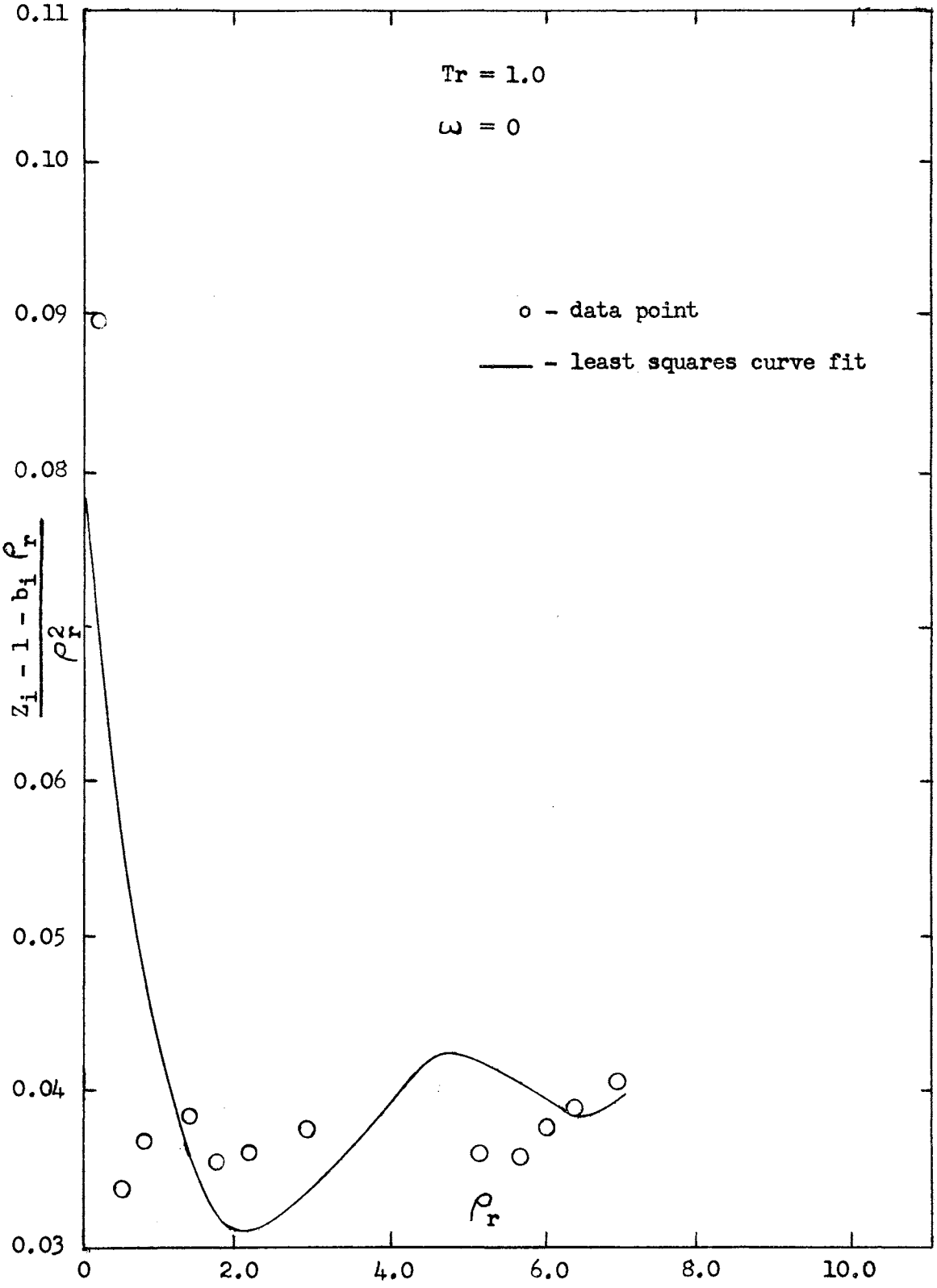

Figure 3

Determination of c_i by Least Squares Curve Fit

in Figure 3. In Figure 3 the data points are plotted, and the fourth degree least squares curve fit to these data drawn in. The intercept of the fitted curve is c_i, in this case 0.08145, but the value is unreliable because of the irregular nature of the plot. The lowest density data point in Figure 3 is very much out of line with the other data points. This is due to the fact that an error in the value of Z_i will be greatly magnified in the ordinate term. In the case mentioned here, a one per cent error in Z_i will give a seventy per cent error in the value of $(Z_i - 1 - b_i \rho_r)/ \rho_r^2$.

The preceding attempt to evaluate c_i was plagued by the irregular nature of the compressibility data, as had been the pressure series evaluations attempted previously. How then, would a value of b_i determined from a curve fit of Pitzer's compressibility compare to b_i calculated from Pitzer's equation for the second virial coefficient? In order to make this comparison values of $(Z_i - 1)/ \rho_r$ were calculated for various ρ_r's at an acentric factor of 0, and a reduced temperature of 1.0. These values are listed in Table 2, and plotted in Figure 4. The fourth degree least squares curve fit is shown as a line in this figure. The intercept of this curve is b_i, in this case -0.3246. This does not compare too well with Pitzer's calculated value of -0.3361.

The attempt to evaluate b_i, described in the preceding paragraph, was not successful, but the plot in that case was smoother than the plot previously obtained in attempting to evaluate c_i. This was encouraging enough to warrant carrying the investigation one step further in this direction. That is, to curve fit a plot of Z_i vs ρ_r for $T_r = 1.0$, and $\omega = 0$. This plot should give a value of 1 as the intercept, and b_i should be the slope at the intercept. These values are listed in

Table 2

Data for b_i Determination by Least Squares Curve Fit.

$T_r = 1.0, \omega = 0$

ρ_r	$\frac{Z_i - 1}{\rho_r}$
0.2146	-0.3169
0.4711	-0.3205
0.7937	-0.3074
1.2539	-0.2887
3.4364	-0.2063
5.1948	-0.1480
5.6000	-0.1339
5.7554	-0.1254
5.9211	-0.1175
6.0790	-0.1104
6.1798	-0.1042
6.2992	-0.0983
6.3882	-0.0928
6.4665	-0.0877
6.5502	-0.0827
6.1157	-0.0780
6.6797	-0.0735
6.7416	-0.0691
6.8223	-0.0649
6.8729	-0.0608
7.0093	-0.0511
7.1225	-0.0418
7.3260	-0.0247
7.5107	-0.0091
7.6336	0.0063
7.7187	0.0215

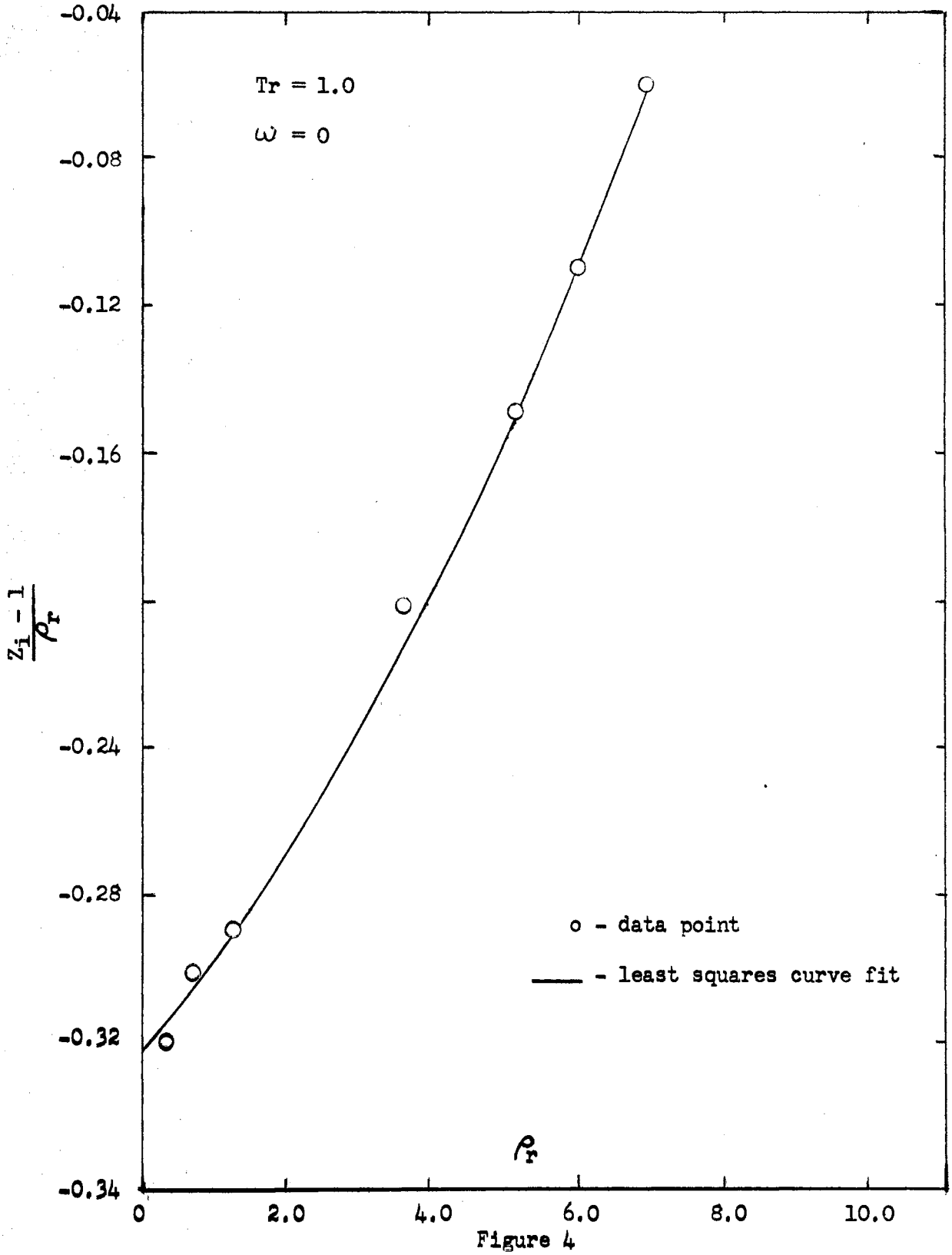

Figure 4

Determination of b_i Using a Generalized Density Basis

Table 3

Data for Plotting Compressibility vs Reduced Density

$T_r = 1.0, \omega = 0$

ρ_r	Z_i
0.2146	0.9320
0.4711	0.8490
0.7937	0.7560
1.2539	0.6380
3.4364	0.2910
5.1948	0.2310
5.6000	0.2500
5.7554	0.2780
5.9211	0.3040
6.0790	0.3290
6.1798	0.3560
6.2992	0.3810
6.3882	0.4070
6.4665	0.4300
6.5502	0.4580
6.1157	0.4840
6.6797	0.5090
6.7416	0.5340
6.8223	0.5570
6.8729	0.5820
7.0093	0.6420
7.1225	0.7020
7.3260	0.8190
7.5107	0.9320
7.6336	1.0480
7.7187	1.1660

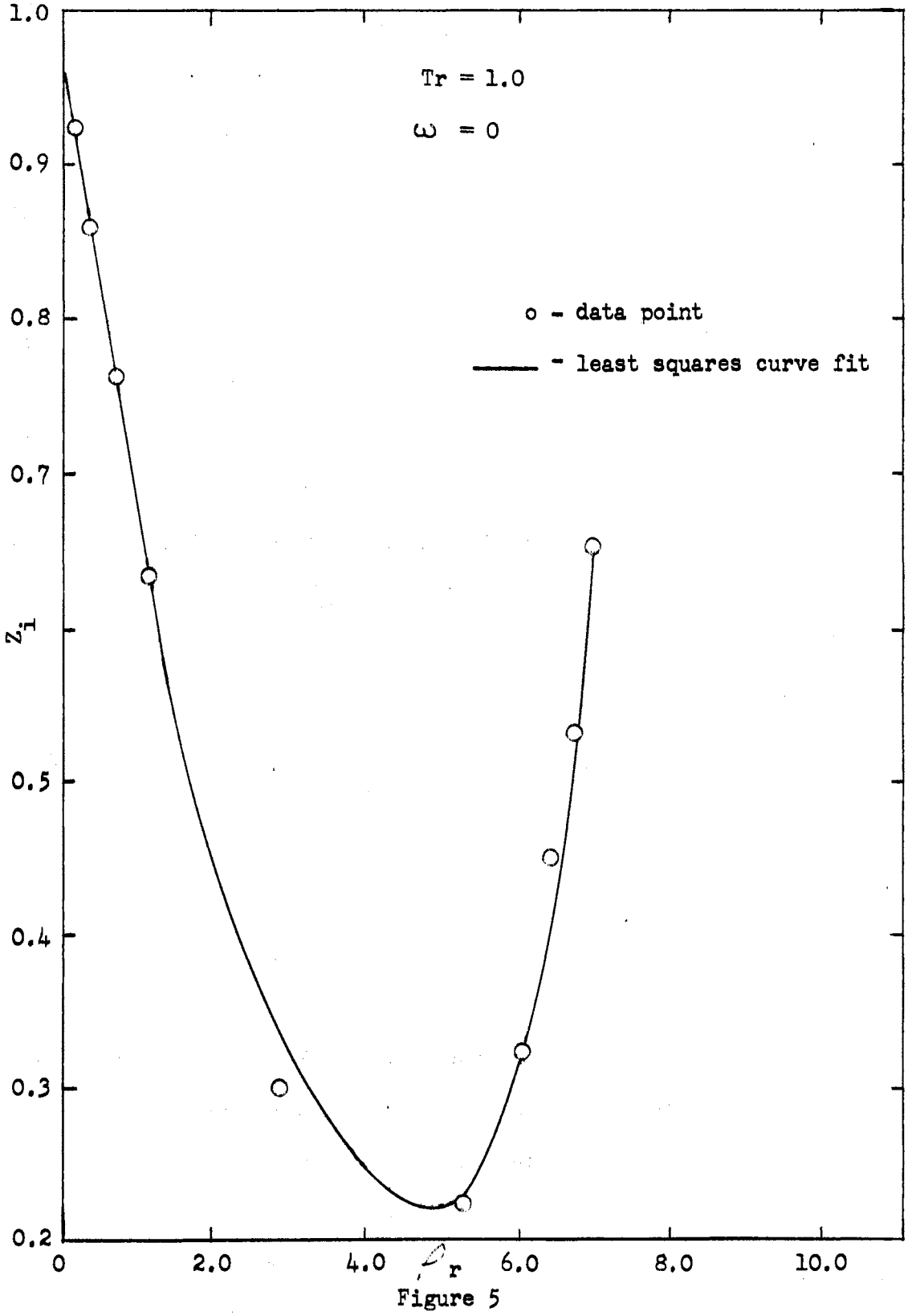

Figure 5

Compressibility as a Function of Generalized Density

Table 3, and plotted in Figure 5. The plot in Figure 5 was smoother than the two previous density series curve fits, shown in Figures 3 and 4, but it was not quite good enough. The intercept was 1.0103, not 1.0000 as it should have been. The slope at the intercept was -0.4017, this does not compare favorably with Pitzer's calculated value of -0.3361. There seems to be some disagreement between Pitzer's second virial equation and his compressibility data, as well as some errors in his data.

The results so far were somewhat discouraging, but there were still some unexplored avenues available. One of these was the use of $(Z_i - 1 - b_i \rho_r)$ and ρ_r as a correlation basis. This is similar to the first density series evaluation attempted, that for c_i. There is a difference though, in this case the ordinate term is not divided by ρ_r^2, which was responsible for compounding the error in the previous case. Values of $(Z_i - 1 - b_i \rho_r)$ were calculated for various ρ_r's at a reduced temperature of 1.0, and an acentric factor of 0. These are listed in Table 4, and plotted in Figure 6. The plot of these values is smooth; much better than any of the previous plots. The calculations were repeated, this time using acentric factor values of 0.1, 0.2, 0.3, 0.4 and 0.5. The plots of these values were also smooth. The plots for the other acentric factors were omitted from the figure for the sake of clarity. The plots would have been practically on top of each other. The curve, incidentally, is an arbitrary, not a fitted curve. It also exhibits the expected approach to zero at zero density, indicating that the compressibility is approaching unity. The promising appearance of this method encouraged a more ambitious undertaking.

The values listed in Table 4, and those for the higher acentric

Table 4

Data for Matrix Inversion Correlation

$T_r = 1.0, \omega = 0$

ρ_r	$Z_i - 1 - b_i \rho_r$
0.2146	.00412
0.4711	.00735
0.7937	.02274
1.2539	.05944
3.4364	.44598
5.1948	.97697
5.6000	1.13216
5.7554	1.21239
5.9211	1.29407
6.0790	1.37216
6.1798	1.43302
6.2992	1.49817
6.3882	1.55408
6.4665	1.60639
6.5502	1.65953
6.1157	1.70615
6.6797	1.75407
6.7416	1.79984
6.8223	1.84996
6.8729	1.89197
7.0093	1.99784
7.1225	2.09587
7.3260	2.28127
7.5107	2.45636
7.6336	2.61365
7.7187	2.76025

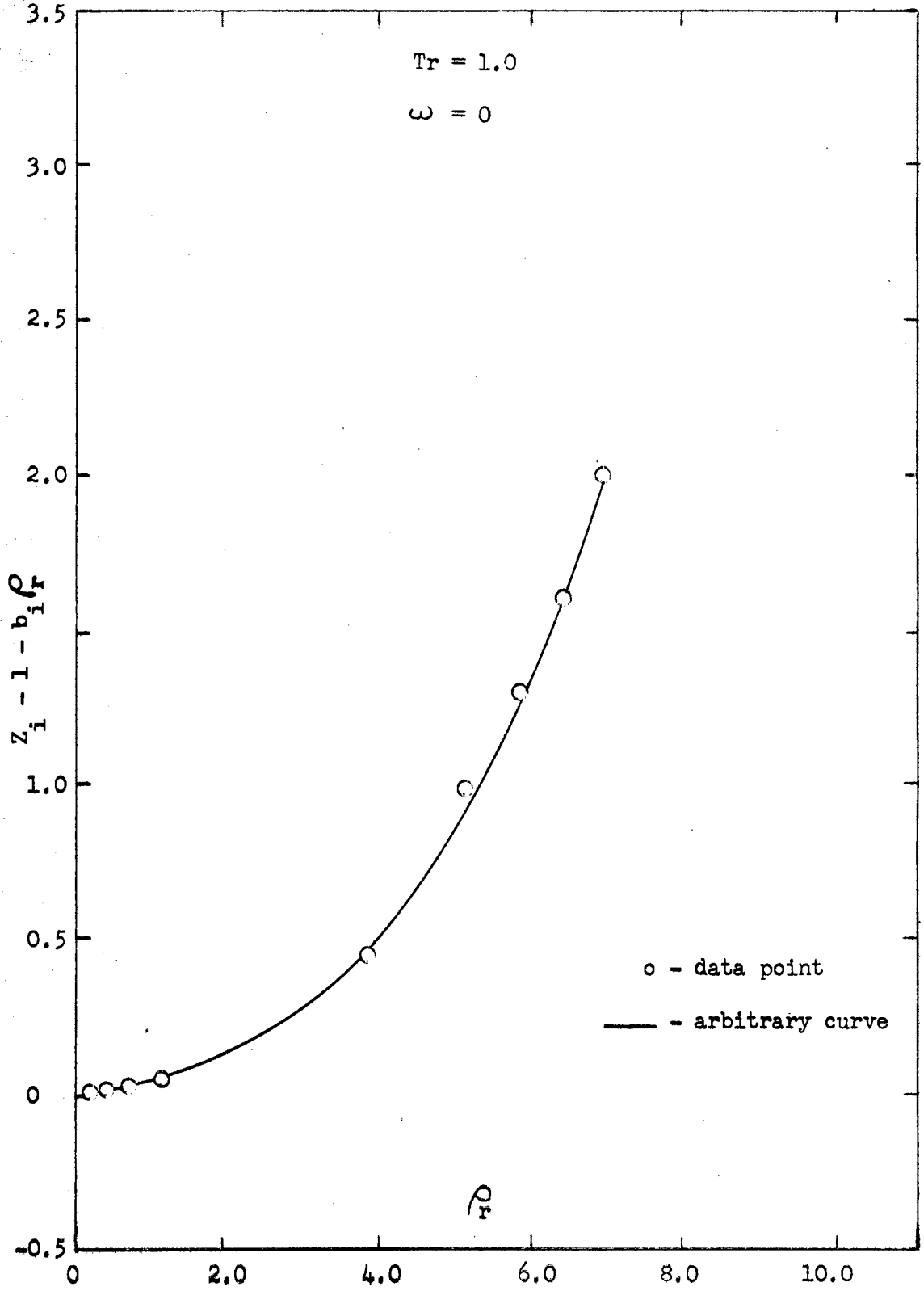

Figure 6

Matrix Inversion Correlation

factor, were processed through a matrix inversion program on the IBM 650 computer. The program gave values for the generalized Leiden virial coefficients c_i, d_i, e_i, f_i and g_i, at $T_r = 1.0$ and acentric factors of 0, 0.1, 0.2, 0.3, 0.4 and 0.5. These values are listed in Table 5, along with the values for Pitzer's b_i, and plotted in Figures 7, 8, 9, 10, 11 and 12, as functions of acentric factor. Pitzer's second virial plots in a straight line, as would be expected since it was calculated from an equation linear in ω. This is shown in Figure 7. The coefficients obtained from the matrix inversion program did not appear to have a definite straight-line dependency upon acentric factor. Although linearity is indicated from the general appearance of the plots, the results were too irregular to allow reliable relationships to be obtained. The 0.4 acentric factor point was omitted in the plots because some malfunction in the calculations gave completely unreasonable results. The other points gave sufficient evidence to justify elimination of this method as a means of obtaining virial coefficient relationships. Even though the plots are irregular, it can be observed that virial coefficients alternately increase, or decrease with acentric factor. The b_i, d_i and f_i values increase with increasing acentric factor, while the c_i, e_i and g_i values decrease with increasing acentric factor. The plot for c_i is the most irregular of the group, and the g_i plot is the least irregular. This demonstrates the lessening of the effect of data error in the higher order terms of the equation of state. By this time it was apparent that there was no possible way to obtain good results from Pitzer's data through curve fitting methods. The data was too irregular to respond to the gentle treatment given it heretofore, so the time had

Table 5

Coefficients from $Z_i - 1 - b_i \rho_r$ vs ρ_r Correlation

$T_r = 1.0$

	b_i*	c_i	d_i	e_i	f_i	g_i
0.0	-0.3361	0.03990	-0.0006116	0.0001826	-0.0001171	0.00001510
0.1	-0.3432	0.04568	-0.0004155	-0.0005608	0.0000305	0.00000567
0.2	-0.3504	0.04443	0.0047865	-0.0025211	0.0002991	-0.00000776
0.3	-0.3575	0.04915	0.0054618	-0.0032050	0.0004103	-0.0000139
0.4	-0.3646	0.2044	-0.1057218	0.0251918	0.0026838	0.0001078
0.5	-0.3718	0.03563	0.0199074	-0.0070847	0.0008204	-0.00003017

*b_i calculated from Pitzer's equation

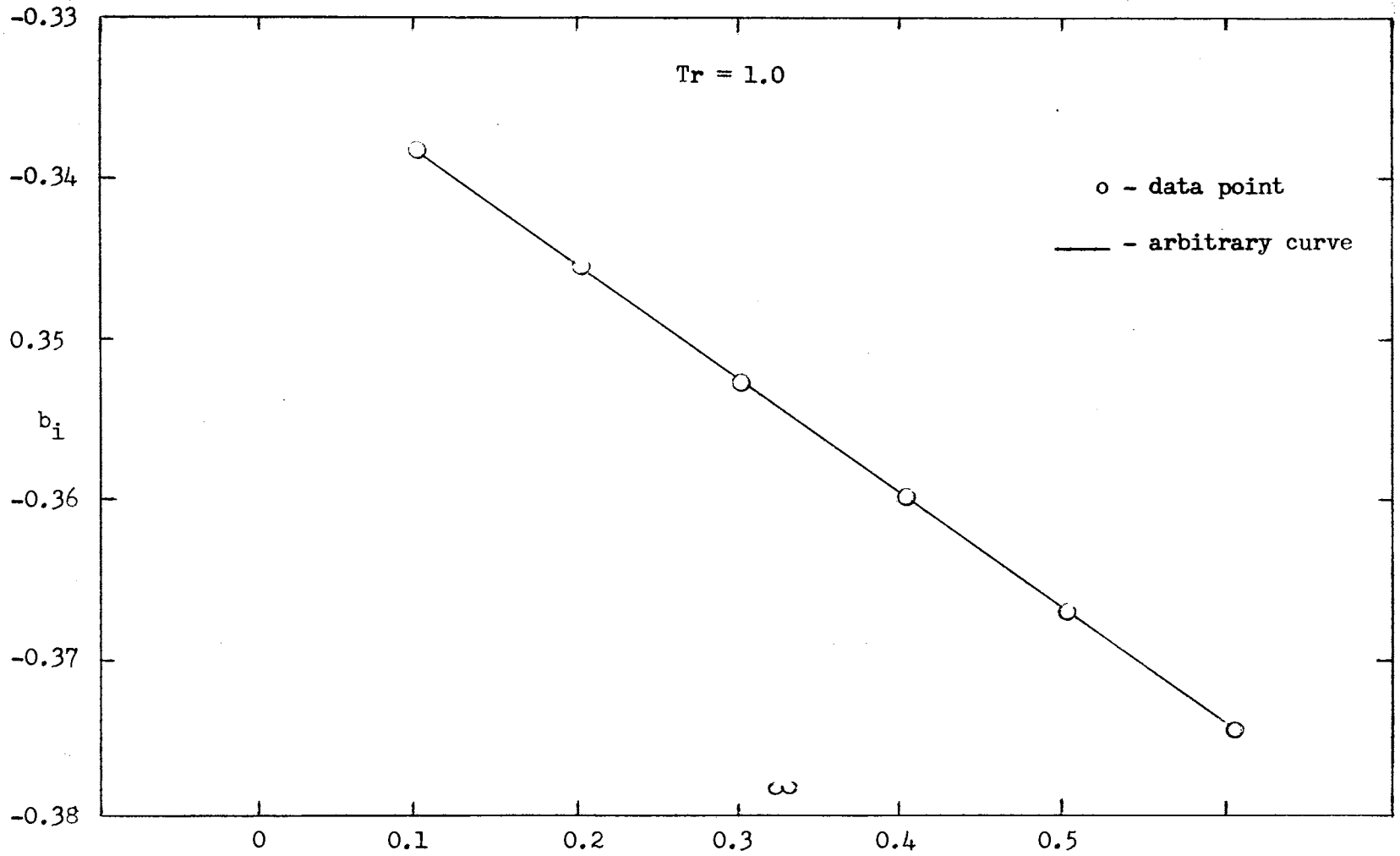

Figure 7

Pitzer's Second Virial as a Function of Acentric Factor

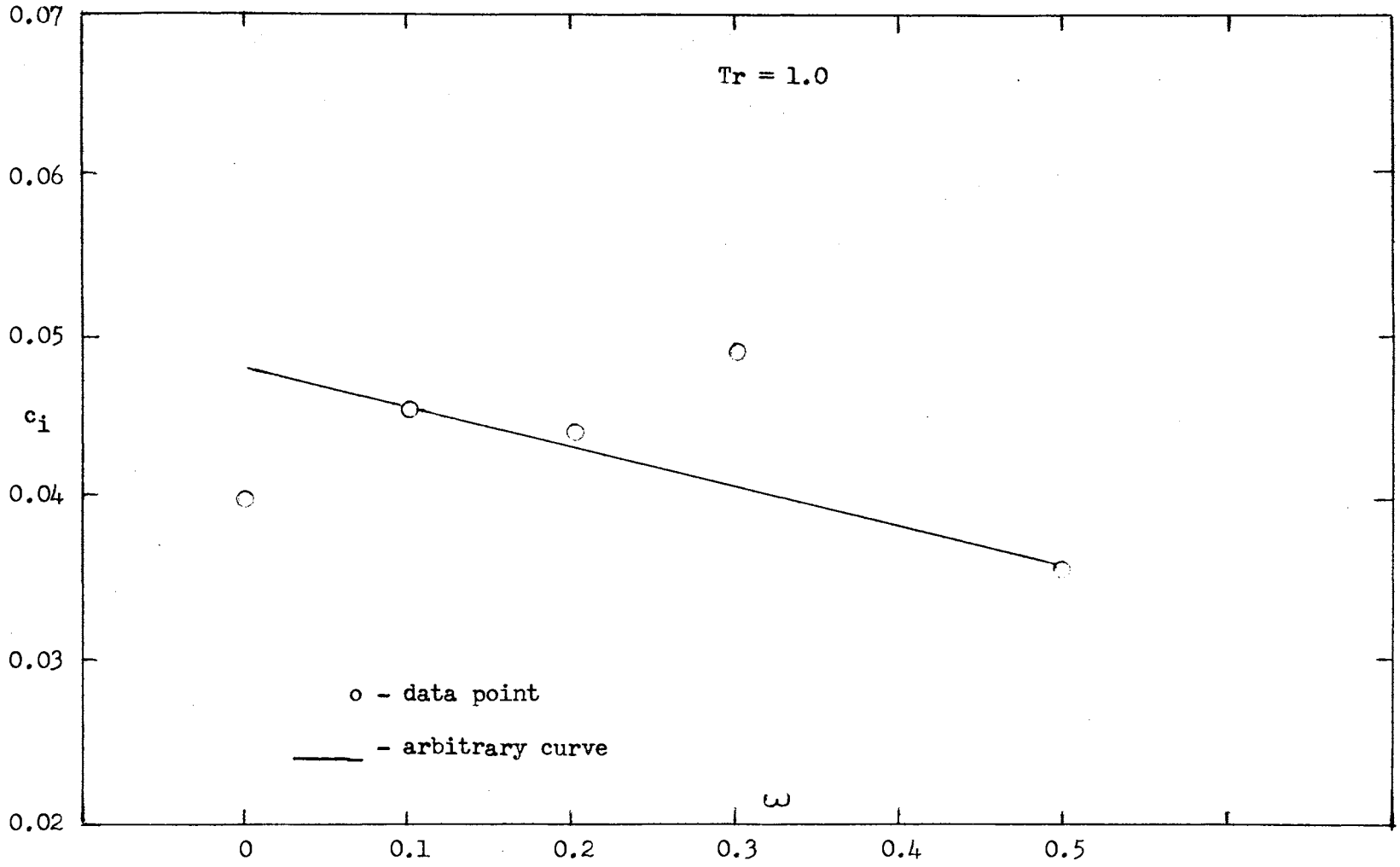

Figure 8

Matrix Inversion c_i as a Function of Acentric Factor

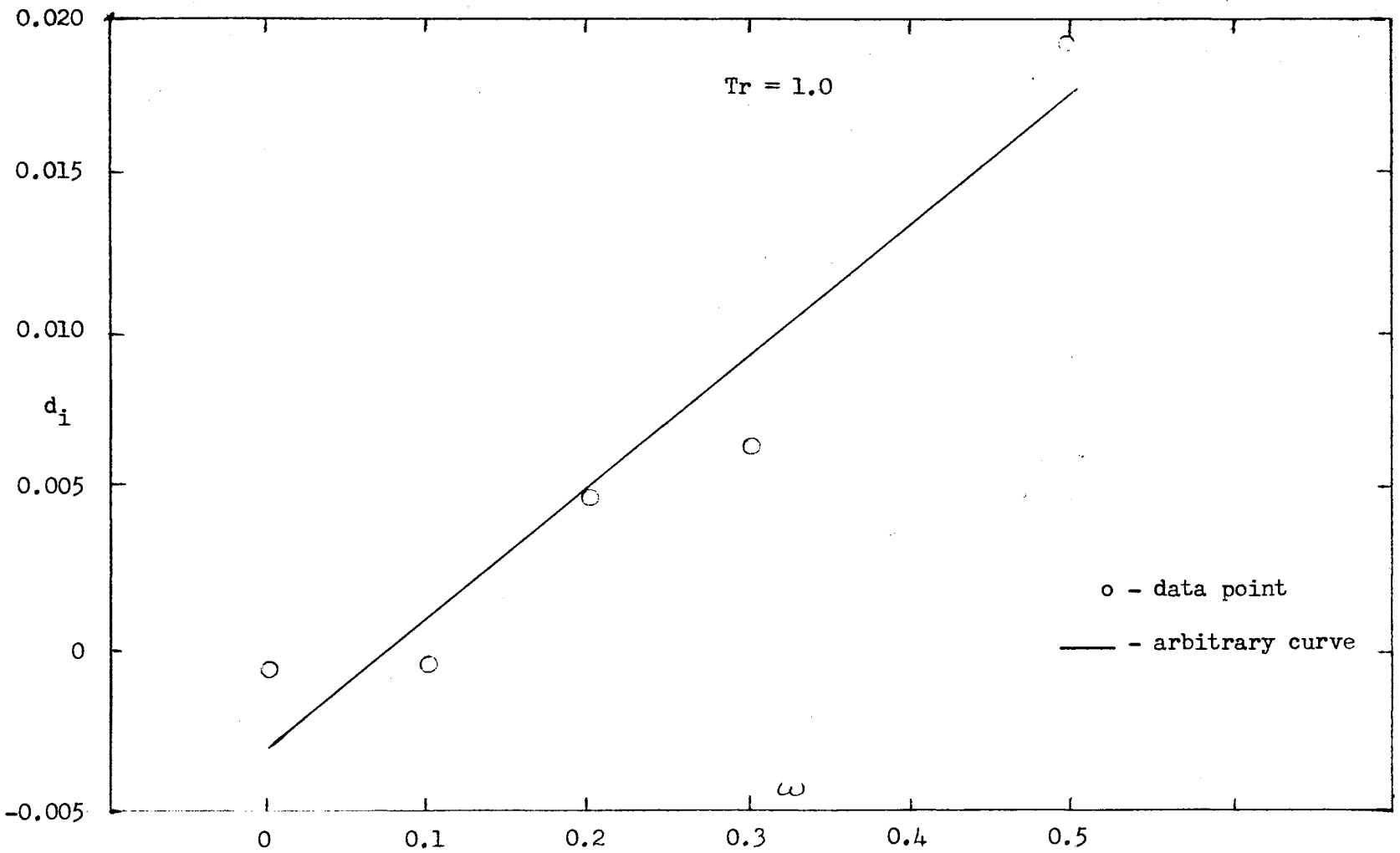

Figure 9

Matrix Inversion d_i as a Function of Acentric Factor

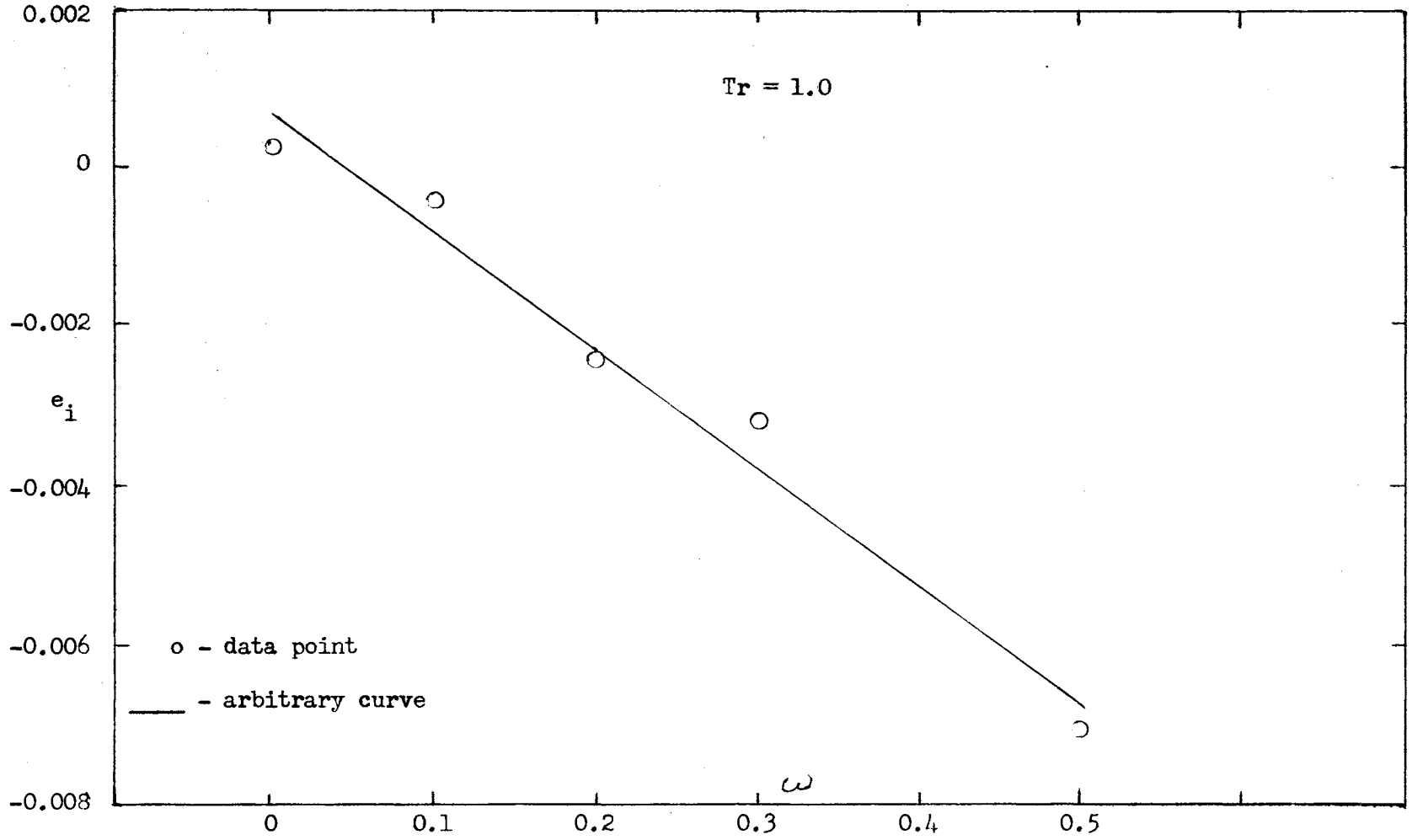

Figure 10

Matrix Inversion e_i as a Function of Acentric Factor

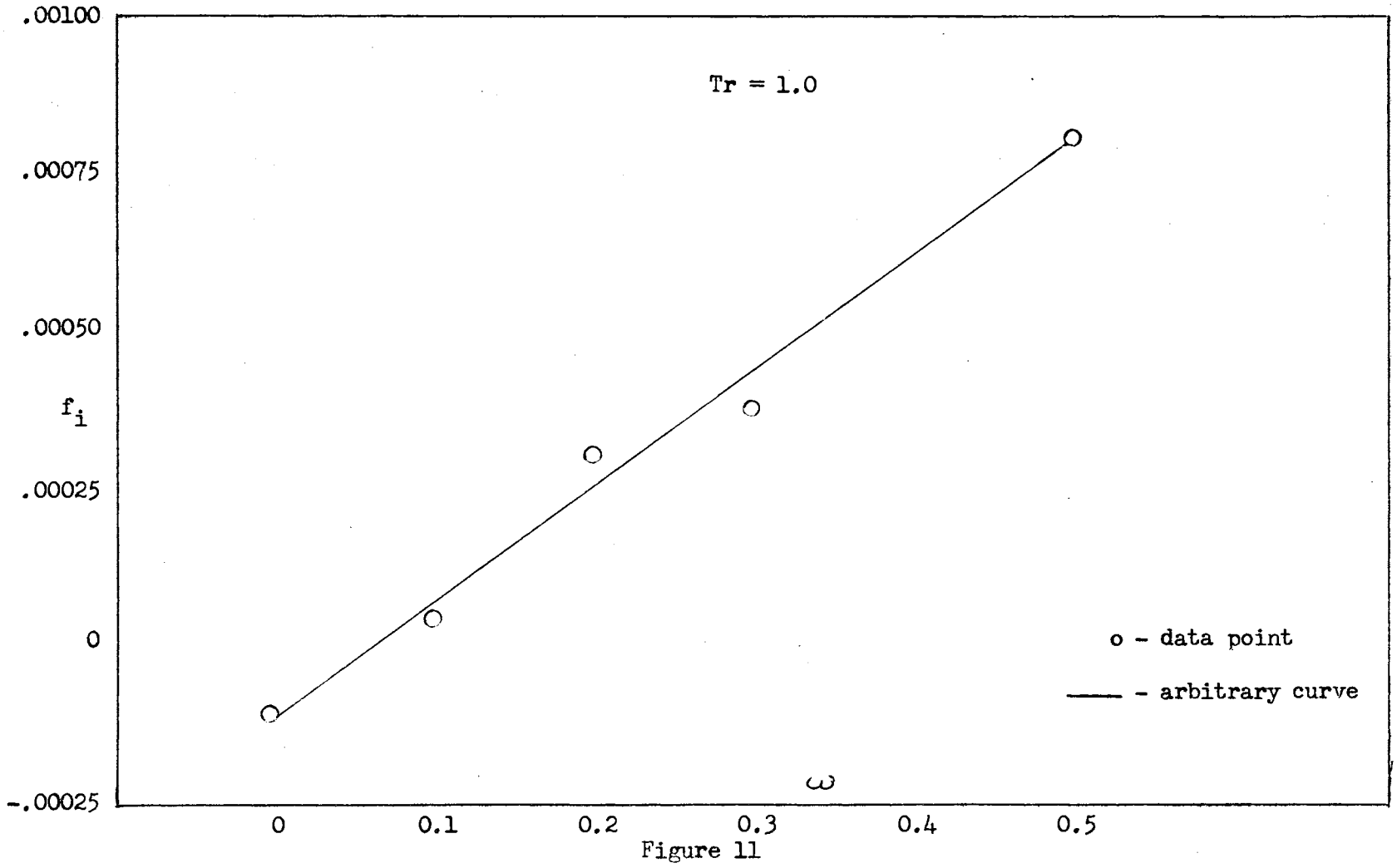

Figure 11

Matrix Inversion f_i as a Function of Acentric Factor

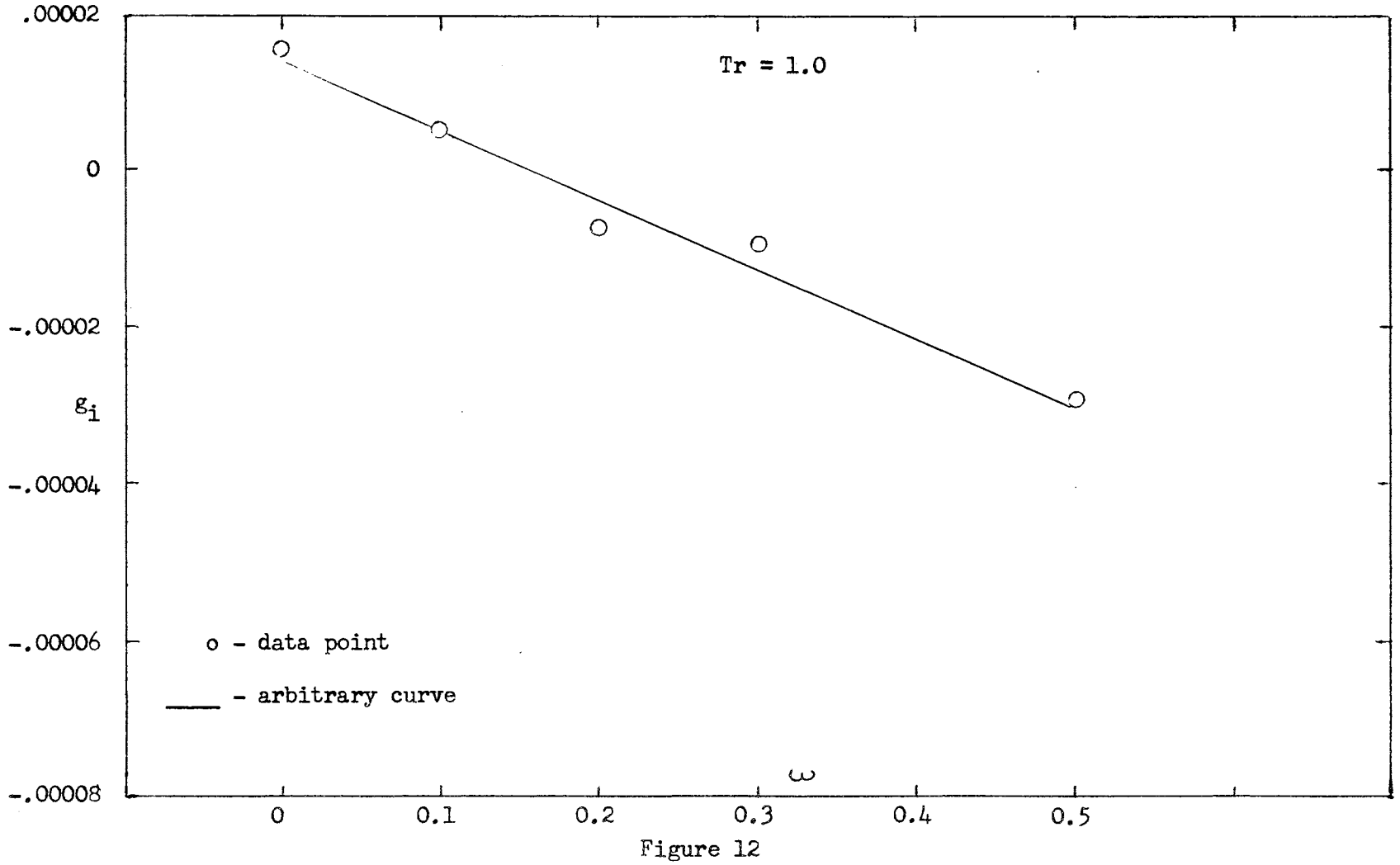

Figure 12

Matrix Inversion g_i as a Function of Acentric Factor

come to apply force. This led to the final step of this investigation.

Density Series Evaluation Via Data Smoothing

Being faced with the prospect of using fair, but not quite good, generalized compressibility data, and a fair. but questionable, second virial coefficient equation required a reevaluation of the situation. How could reasonable results be obtained from this information? The method used in Figure 4, i.e., plotting $(Z_i - 1)/\rho_r$ vs ρ_r, seemed to offer the best possibility. This time, however, Pitzer's value for b_i was to be used as the intercept. Instead of a curve fit, the curve was to be drawn in the smoothest manner to fit the data, and to intercept at Pitzer's value of b_i. The slope of this curve would be c_i. Values of ρ_r and $(Z_i - 1)/\rho_r$ were calculated for all of Pitzer's compressibility data at, and above the critical temperature. These were calculated for acentric factor values of 0, 0.1, 0.2, 0.3 and 0.4. The plot for the acentric factor of 0 is shown in Figure 13. This is typical of the plots obtained for the other acentric factors, although they did become more irregular at the higher acentric factor values. This method, as such, was not applicable for temperatures below the critical, so this thesis does not show any values in this region. Pitzer's second virial seemed to give reasonable intercept values for T_r values through 2.0, but above this Pitzer's values were ignored because they were too high and would not have given the desired parametric shape to the isotherms in this region. The points corresponding to $P_r = 1.0$ are shown on the isotherms, the portion of the curve up to this point can probably be adequately expressed by a quadratic expression involving the second and third coefficients only. An expression

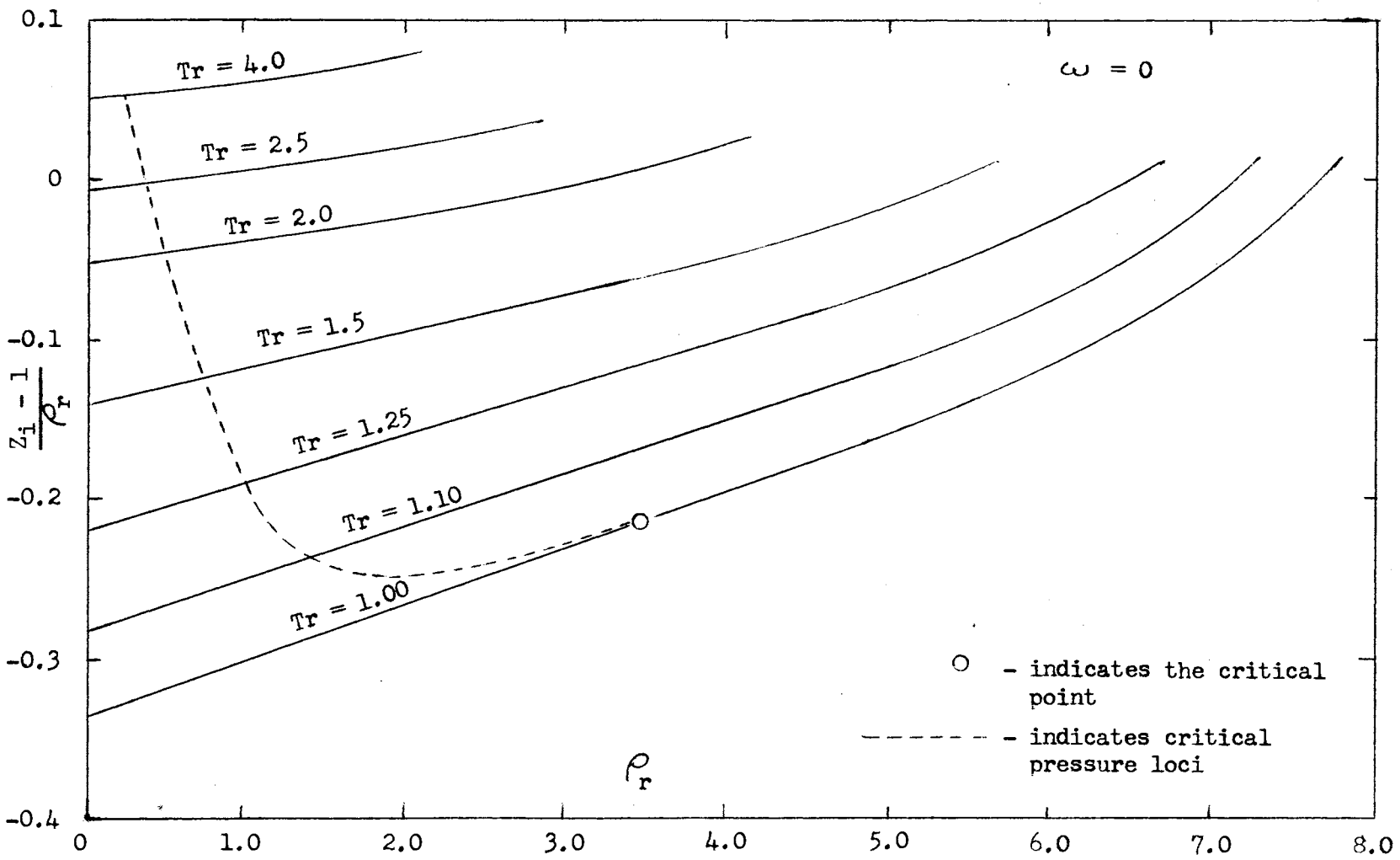

Figure 13

Determination of c_i From Slope of Smoothed Curve

applicable over the entire pressure range would require the use of more virials.

The c_i values obtained from the slopes were then plotted vs $1/T_r$ and smoothed curves were drawn for each acentric factor, as illustrated in Figure 14. A smoothed plot of Pitzer's second virial over the same temperature range is shown in Figure 15.

Table 6 shows values of b_i as determined from Pitzer's equation, and b_i as determined from the intercept in Figure 13, also it shows the value of c_i as read from the smoothed curves in Figure 14. These are all for an acentric factor of zero. Table 7 gives the same listing for an acentric factor of 0.40. Figure 14 shows c_i to apparently be a linear function of ω, so that a correlation for c_i can be made by curve-fitting c_i as a function of T_r and P_r at acentric factors of 0 and 0.4, then determining the final correlation from these two functions. The result would be similar to the equation developed by Pitzer.

Using Tables 6 and 7 to correlate c_i in the manner described above gave the following relationship for the Leiden generalized third virial coefficient.

$$c_i = -(0.0043 + 0.0588\omega) + (0.0516 + 0.239\omega)/T_r - (0.0315 + 0.440\omega)/T_r^2 + (0.0225 + 0.2688\omega)/T_r^3 \quad \text{(III-10)}$$

The unsatisfactory behavior of Pitzer's second virial at the higher reduced temperatures prompted a reevaluation of this equation. It was made using the b_i values in Tables 6 and 7. The new equation for the Leiden generalized second virial coefficient obtained was

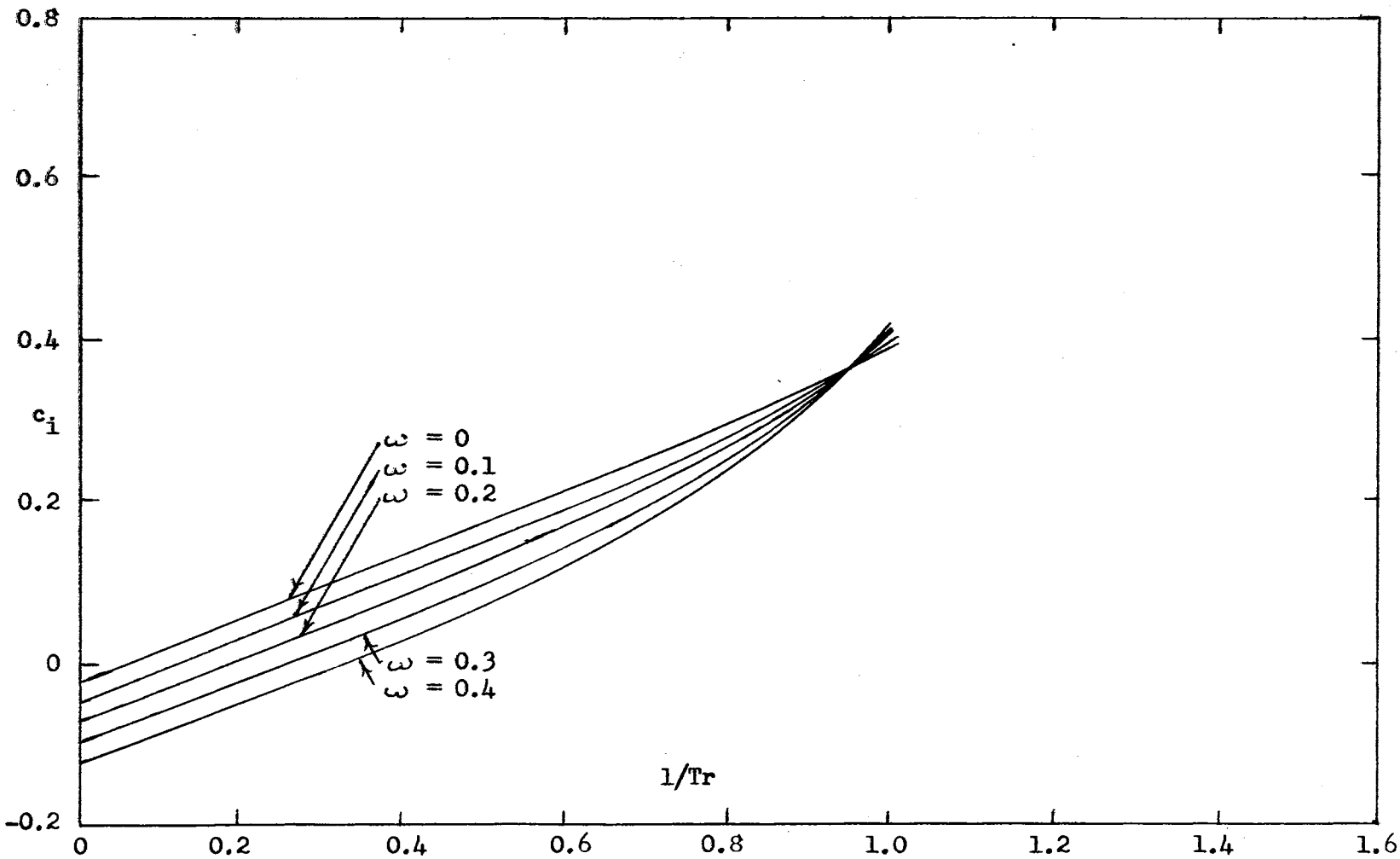

Figure 14

Smoothed Third Virial Coefficient Curves

Table 6

Generalized Leiden Virial Coefficients for $\omega = 0$

Tr	Pitzer's b_i	Intercept b_i	Figure 14 c_i
1.00	-.3361	-.3361	.0381
1.05	-.3058	-.3058	.0357
1.10	-.2790	-.2790	.0337
1.15	-.2551	-.2551	.0316
1.20	-.2336	-.2336	.0298
1.25	-.2143	-.2143	.0282
1.30	-.1968	-.1968	.0268
1.40	-.1662	-.1662	.0245
1.50	-.1406	-.1406	.0227
1.60	-.1188	-.1188	.0212
1.70	-.1000	-.1000	.0198
1.80	-.0836	-.0836	.0185
1.90	-.0693	-.0693	.0174
2.00	-.0566	-.0566	.0164
2.50	-.0104	-.0104	.0127
3.00	.0186	.0170	.0102
3.50	.0386	.0350	.0083
4.00	.0531	.0466	.0070

Table 7

Generalized Leiden Virial Coefficients for $\omega = 0.4$

Tr	Pitzer's b_i	Intercept b_i	Figure 14 c_i
1.00	-.3646	-.3646	.0347
1.05	-.3183	-.3183	.0341
1.10	-.2783	-.2783	.0307
1.15	-.2436	-.2436	.0282
1.20	-.2131	-.2131	.0261
1.25	-.1826	-.1826	.0241
1.30	-.1624	-.1624	.0225
1.40	-.1220	-.1220	.0196
1.50	-.0892	-.0892	.0172
1.60	-.0622	-.0622	.0152
1.70	-.0397	-.0397	.0146
1.80	-.0206	-.0206	.0121
1.90	-.0043	-.0043	.0107
2.00	.0097	.0097	.0096
2.50	.0578	.0567	.0053
3.00	.0855	.0801	.0026
3.50	.1031	.0971	.0004
4.00	.1152	.1091	-.0012

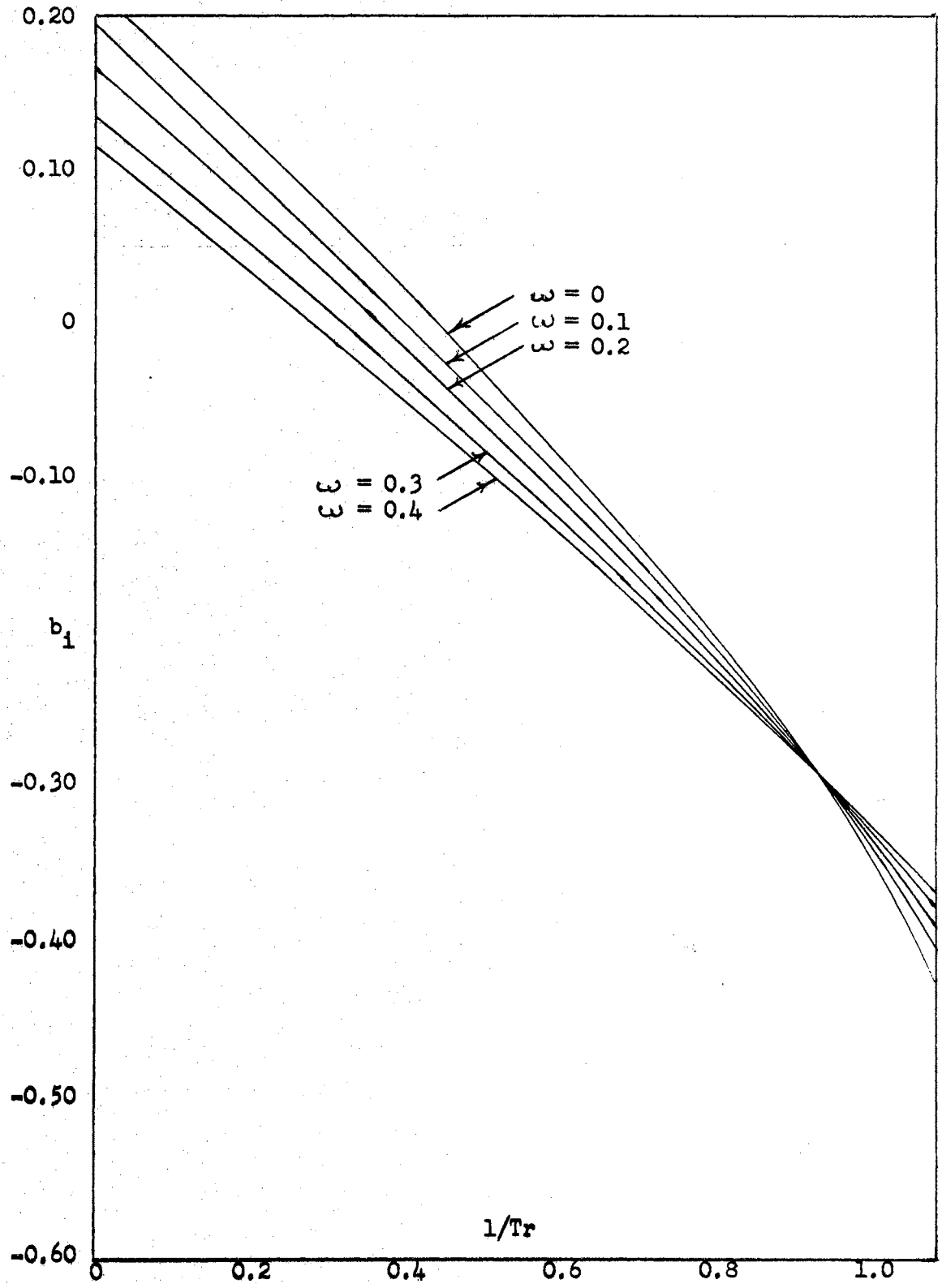

Figure 15

Pitzer's Second Virial as a Function of Reciprocal Temperature

$$b_i = (0.1206 + 0.077\omega) - (0.229 - 0.396\omega)/T_r$$
$$-(0.2946 + 0.3443\omega)/T_r^2 + (0.0603 - 0.201\omega)/T_r^3 \qquad \text{(III-11)}$$

Equations (III-10) and (III-11) were used in evaluating both the Berlin and Leiden equations for the imperfection pressure correction term in Chapter IV. The Berlin coefficients were calculated using equations (III-8) and (III-9) with equations (III-11) and (III-10).

CHAPTER IV

COMPARISON OF DENSITY INTEGRAL AND PRESSURE INTEGRAL EVALUATIONS

The imperfection pressure correction term was evaluated by the Pressure Integral and Density Integral methods (Equations (II-38) and (II-59). Both of these evaluations made use of the two virial coefficient equations developed in Chapter III. The range of the reduced temperatures used in the evaluation was from 1.0 to 4.0, and the reduced pressures from 0.1 to 10.0. The imperfection pressure correction term was evaluated at an acentric factor of zero to determine the simple fluid value, and at an acentric factor of 0.4 to allow the determination of deviation from the simple fluid value. The simple fluid value, $\ln \theta_i^o$, the value at an acentric factor of ω, $\ln \theta_i'$ are related through[1]

$$\ln \theta_i = \ln \theta_i^o + \omega \ln \theta_i' \qquad \text{(IV-1)}$$

Values for $\ln \theta_i$ and $\ln \theta_i^o$ were calculated, then the deviation value was determined using

$$\ln \theta_i' = (\ln \theta_i - \ln \theta_i^o)/\omega \qquad \text{(IV-2)}$$

Knowing $\ln \theta_i$ and $\ln \theta_i^o$ allowed calculation of K_I^o and K_I' by using

---

[1]Later work prior to the publication of this thesis has disproved the validity of this mathematical model.

Equations (I-3), (I-5) and (I-6).

The Pressure Integral method, as can be seen from Equation (II-39), is a straightforward calculation. The reduced liquid volume was evaluated by the method mentioned in Appendix B, and the reduced vapor pressure, p_r^o, was evaluated as a function of reduced temperature, also given in Appendix B. The virial coefficients were evaluated by using Equations (III-11) and (III-8) for B_i'', and Equations (III-10) and (III-9) for C_i''. The evaluation was made on the IBM 1620 computer with a program designed to accept acentric factor, reduced temperature, and reduced pressure as data values.

The Density Integral method, requires a trial-and-error solution of Equation (II-57) to determine the values of the compressibility factor, Z_i, and the reduced density, ρ_r, at the system and vapor pressures. The virial coefficient was evaluated from Equations (III-10) and (III-11) and the reduced vapor pressure by the method given in Appendix B. The iterative procedure used in the trial-and-error solution was that of interval halving; Newton's method was attempted but it gave erroneous results, particularly at the higher pressures. The tolerance used in the evaluations was 0.00001, applied to Z_i.

The results of the Density Integral method evaluation using the second and third virial coefficients are shown in Figures 16, 17, 18 and 19. At the critical temperature ($T_r = 1.0$) the calculations were terminated at $P_r = 8.0$, an attempt to obtain convergence at $P_r = 9.0$ was unsuccessful after thirty minutes of iteration. Another convergence method, or perhaps a faster machine will be necessary to obtain values at the critical temperature for extremely high pressure.

Figure 16 illustrates the constant temperature effect of pressure upon the simple fluid imperfection pressure correction term. The isotherms on the semi-log plot show the correction term to increase with temperature, and to decrease with pressure. The rate of decrease with pressure is less constant at the lower temperatures.

Figure 17 illustrates the deviation from a simple fluid of the imperfection pressure correction term. The isotherms on the semi-log plot show the deviation to increase slightly with pressure, this effect becomes more pronounced at the higher temperatures. The deviation value is also much greater at the higher temperatures. In other words, the deviation of the imperfection pressure correction term for a component from that of a simple fluid increases rapidly with temperature, and to a lesser degree with pressure.

Figure 18 illustrates the constant temperature effect of pressure on the ideal K-values. The effect of increasing pressure becomes more noticeable at the lower temperatures. An increase of K-value with temperature is observed up to a reduced temperature of 3.0, then a retrogression occurs, the $T_r = 4.0$ isotherm dropping below the $T_r = 2.0$ isotherm. Isotherm retrogression at the extremely high temperatures has been previously observed (4) and should perhaps be expected in this evaluation. At higher temperatures the isotherm lines tend to become straighter, this illustrates the approach to ideality of behavior. In the calculations it was observed that if finer increments of temperature had been used the plots of adjacent isotherms would cross. This indicates a need for additional virial coefficients to obtain proper evaluations, particularly at the higher pressures.

Figure 19 illustrates the constant temperature effect of pressure

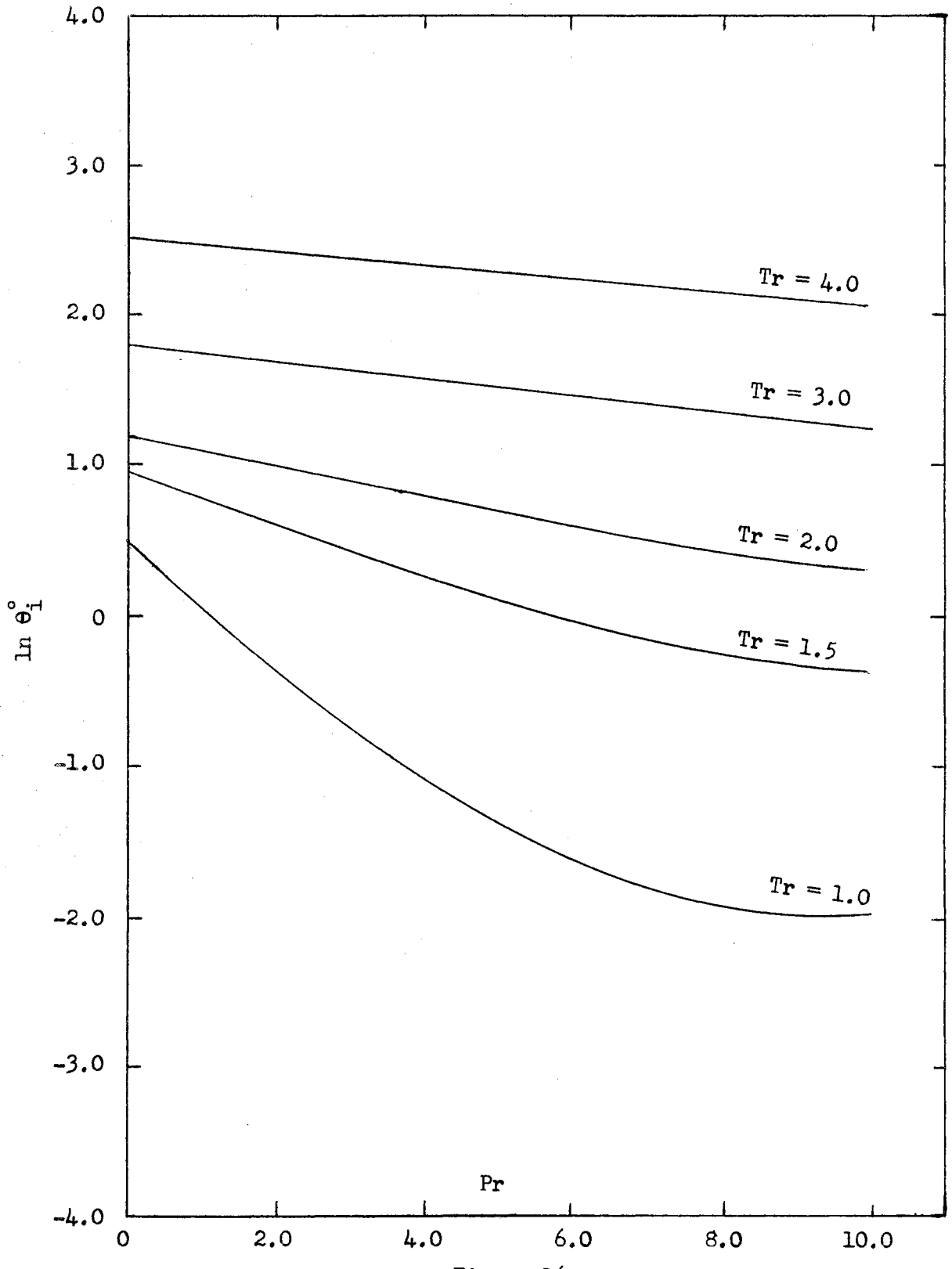

Figure 16

Density Integral Simple Fluid Imperfection Pressure Correction Term

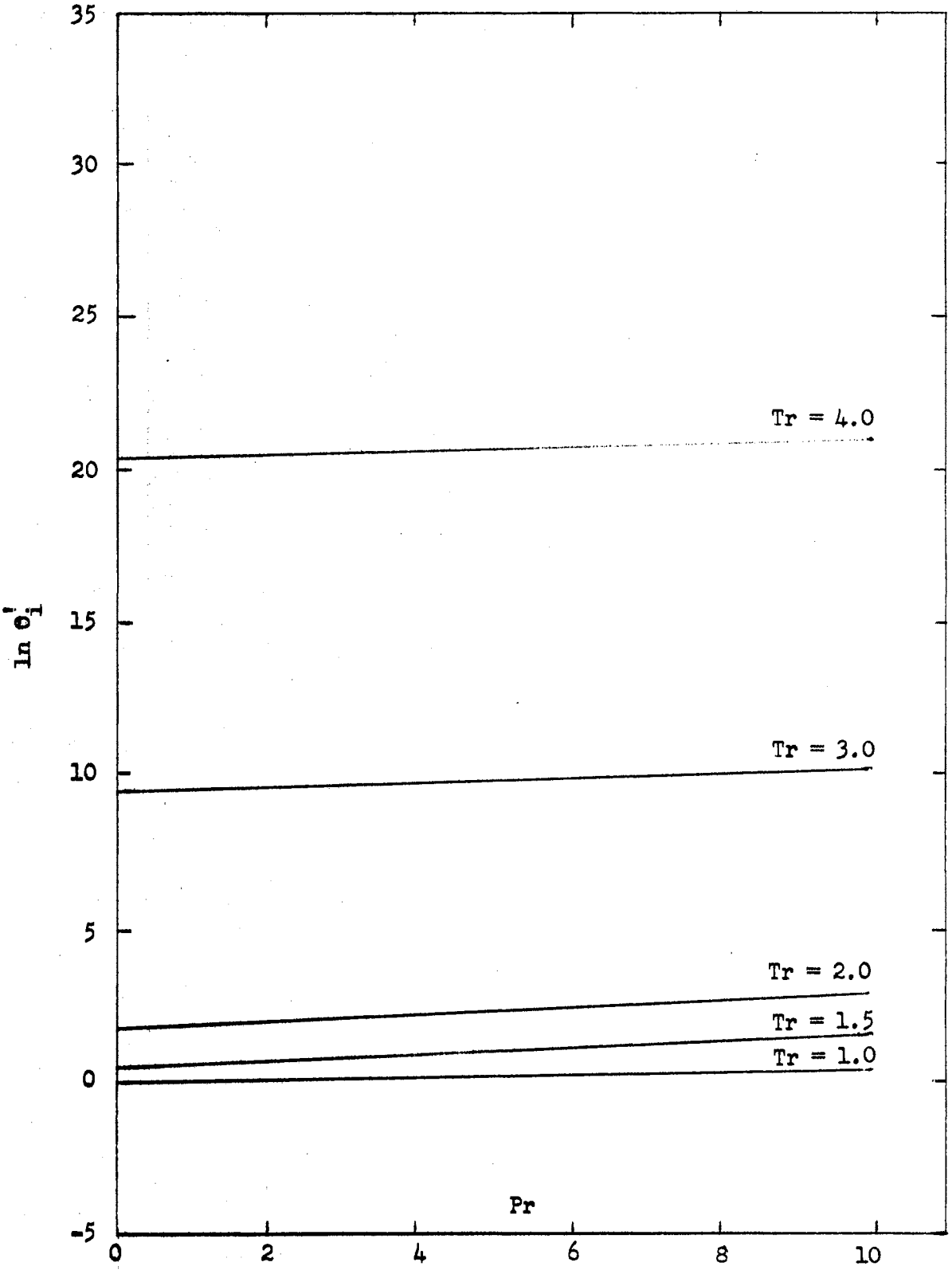

Figure 17

Density Integral Deviation From Simple Fluid
Imperfection Pressure Correction Term

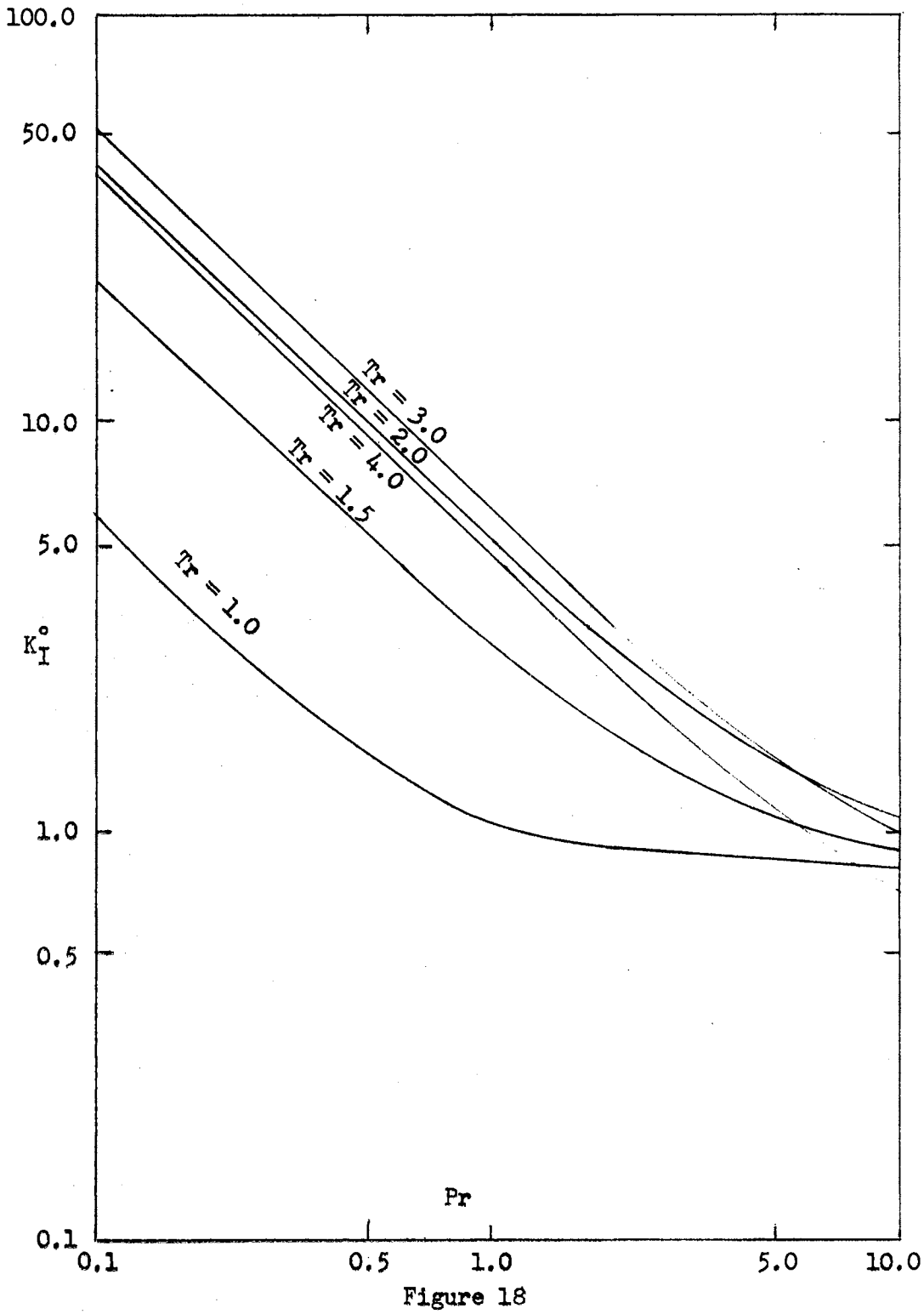

Figure 18

Density Integral Simple Fluid Ideal K-Value

upon the deviation of the ideal K-value from that of a simple fluid. The isotherms show the deviation to decrease with both pressure and temperature, and the decrease to become more pronounced at the higher pressures, until a T_r of 1.5 is reached, then the deviation begins to decrease with increasing temperature. At the higher temperatures the deviation becomes very small, as is indicated by the fact that the $T_r = 4.0$ isotherm was too low to appear on the graph. This further illustrates the approach to ideal behavior at the higher temperatures.

A comparison of Figures 18 and 20 gives an indication of the relative reliability of the Density Integral and Pressure Integral methods of evaluating ideal K-values. In both cases the critical isotherm shows the same behavior up to the critical pressure, but above this the Pressure Integral plot drops to a minimum value then increases rapidly to an ideal K-value beyond the scope of the graph. The $T_r = 1.5$ isotherm is located lower in the Pressure Integral evaluation than in the Density Integral and exhibits a more irregular behavior by recurving and crossing the isotherms. The isotherms for the high temperatures are fairly straight for both the Density Integral and Pressure Integral evaluations, but differences are observed in the K_i^o values, the isotherm spacings, and the amount of retrogression observed in the two cases. The retrogression of the $T_r = 4.0$ isotherm is observed in the Pressure Integral plot as it was in the Density Integral but it was not as extreme in the former case. Judging solely on the basis of the behavior of the lower isotherms it could be said that the Density Integral evaluation is better than the Pressure Integral evaluation. Accepting this, it could be concluded that the Density Integral method does a better job in general in ideal K-value

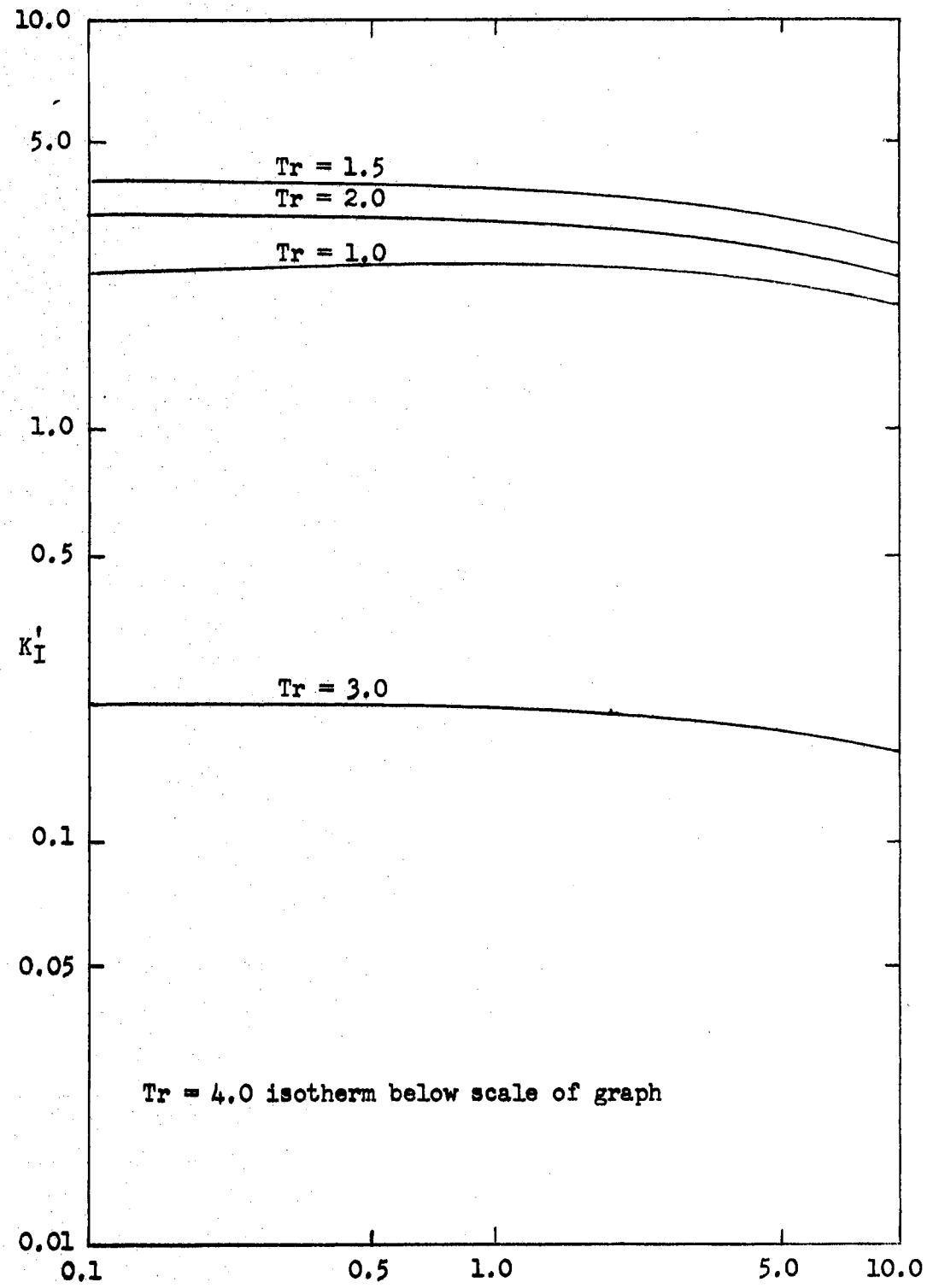

Figure 19

Density Integral Deviation from Simple Fluid Ideal K-Value

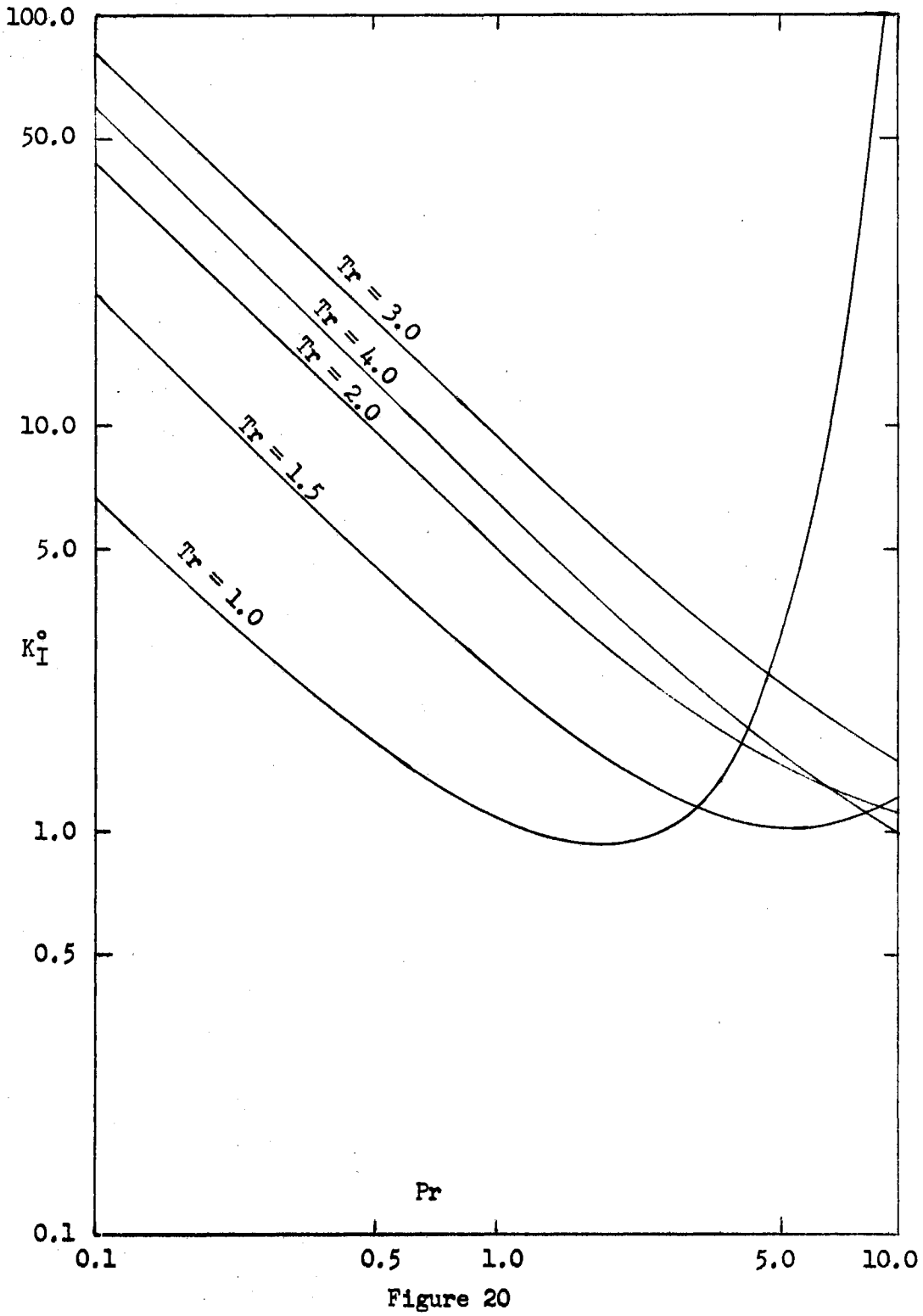

Figure 20

Pressure Integral Simple Fluid Ideal K-Value

evaluation. The Pressure Integral evaluation high pressure behavior at the lower temperature could possibly be improved by using additional virials, but this would merely point out the better economics of the Leiden evaluation, i.e., getting the best evaluation using the least number of terms. The higher temperature behavior of the Berlin evaluation would still be questionable, even with additional virials.

CHAPTER V

VAPOR PHASE ACTIVITY COEFFICIENT EVALUATION

An expression for the vapor phase activity coefficient of a fluid mixture component can be obtained by rearranging Equation (I-2)

$$\gamma_i^V = \gamma_i^L \frac{K_I}{K_i} \qquad \text{(V-1)}$$

The ideal K-value, K_I, can be calculated using the Leiden method developed in Chapter IV and the actual K value, K_i, can be calculated from experimental data. The remaining term, γ_i^L, can be calculated from the Scatchard-Hildebrand (7) equation for the liquid activity coefficient. This equation is given in Appendix B.

Experimental data from two ternary mixtures was chosen for vapor phase activity coefficient evaluation. The first (5) was a methane, ethane, n-pentane mixture at 100°F and pressures from 500 to 2,000 psia. The second (6) was a methane, propane, n-pentane mixture at 220°F and pressures from 500 to 1,500 psia. The data are located in Tables 8 and 9. The γ_i^V values calculated from the data are listed in Tables 10 through 13 and plotted in Figures 21 through 24 in the form of isobaric plots of the liquid activity coefficient vs. mol fraction for the two lighter components. The ternary mixtures chosen were such that vapor-liquid equilibrium for the lighter components could be obtained under conditions not possible for binary mixtures

Table 8

Ternary Data for a Methane, Ethane, n-Pentane Mixture (5)

Temperature = 100°F.

Pressure	Methane		Ethane		n-Pentane	
Psi	Gas	Liquid	Gas	Liquid	Gas	Liquid
	0.904	0.154	0.0377	0.0284	0.0583	0.818
	0.652	0.115	0.297	0.223	0.0519	0.662
500	0.517	0.0947	0.431	0.327	0.0511	0.578
	0.275	0.0550	0.681	0.514	0.0440	0.431
	0.000	0.0000	0.965	0.736	0.0349	0.264
	0.762	0.263	0.188	0.211	0.0499	0.526
	0.674	0.246	0.282	0.314	0.0454	0.440
1000	0.596	0.237	0.360	0.396	0.0443	0.368
	0.598	0.224	0.405	0.444	0.0468	0.331
	0.483	0.214	0.473	0.515	0.0438	0.271
	0.394	0.198	0.562	0.602	0.0441	0.200
	b0.196	0.196	0.758	0.759	0.0450	0.0451
	0.814	0.420	0.125	0.152	0.0608	0.428
	0.689	0.412	0.244	0.291	0.0670	0.297
1500	0.588	0.413	0.334	0.378	0.0779	0.209
	b0.461	0.462	0.443	0.443	0.0953	0.0948
	0.899	0.580	0.0173	0.0217	0.0833	0.399
2000	0.801	0.587	0.0981	0.116	0.101	0.297
	0.763	0.599	0.121	0.140	0.116	0.261

b--single phase present

Table 9

Ternary Data for a Methane, Propane. n-Pentane Mixture (6)

Temperature = 220°F

Pressure	Methane		Propane		n-Pentane	
Psi	Gas	Liquid	Gas	Liquid	Gas	Liquid
	0.571	0.091	0.190	0.160	0.239	0.749
	0.345	0.062	0.451	0.377	0.204	0.561
500	0.329	0.061	0.472	0.389	0.199	0.550
	0.170	0.043	0.666	0.570	0.164	0.387
	0.059	0.010	0.809	0.697	0.132	0.293
	0.714	0.228	0.106	0.138	0.180	0.634
	0.669	0.223	0.155	0.192	0.176	0.585
1000	0.566	0.214	0.264	0.306	0.170	0.480
	0.521	0.208	0.318	0.370	0.161	0.421
	0.397	0.197	0.463	0.516	0.140	0.287
	0.689	0.390	0.108	0.133	0.203	0.477
1500	0.598	0.388	0.194	0.228	0.208	0.384
	0.542	0.422	0.239	0.262	0.219	0.316

of the two. Each mixture contained methane as the lightest component and normal pentane as the heaviest. In each case methane was considerably above its critical temperature, while the next lighter component was very near to its critical temperature.

Figures 21 and 22 were obtained from the methane, ethane, n-pentane data. Figure 21 shows the vapor phase activity coefficient of methane in this mixture as a function of the mole fraction of methane in the vapor phase. The system temperature of 100°F corresponds to a reduced temperature of 1.630 and the pressures of 500, 1000, 1500 and 2000 psia correspond to reduced pressures of 0.743, 1.486, 2.229 and 2.971. The plots should converge to a γ_i^V value of 1.0 for the pure component; they do not do this, in fact they do not converge at all. This indicates that a flaw exists somewhere in the calculations, liquid volume evaluation, or the reduced vapor pressure evaluation. Possibly an additional virial would help. In Figure 22 the same plots are made for ethane in the same mixture. In this case the system temperature corresponds to a reduced temperature of 1.018, and the pressures correspond to reduced pressures of 0.697, 1.394, 2.092 and 2.789. These plots show even less tendency to converge, and are farther from a pure component value of 1.0. Also, a retrogression occurs at the higher pressures. An explanation for the worse behavior would be the lower reduced temperature which, incidentally, is near critical.

Figures 23 and 24 were obtained from the methane, propane, n-pentane data. Figure 23, for methane, is for a system temperature of 220°F, or a reduced temperature of 1.980. The system pressures of 500, 1000, and 1500 psia correspond to reduced pressures of 0.743, 1.486, and 2.229. The plots appear to converge to a value of 1.249 instead of 1.0

Table 10

Data for Figure 21, γ_i^V vs Mol Friction Methane in a Methane, Ethane, n-Pentane Mixture

Temperature = 100°F, T_r = 1.630

Pressure Psi	Reduced Pressure	Methane Vapor-Phase Mol Fraction	Methane Vapor-Phase Activity Coefficient
500	0.743	0.000	1.002
		0.275	0.885
		0.517	0.811
		0.652	0.782
		0.904	0.755
1000	1.486	0.196	2.598
		0.394	1.307
		0.483	1.152
		0.548	1.064
		0.596	1.035
		0.674	0.950
		0.762	0.899
1500	2.229	0.461	2.018
		0.588	1.415
		0.689	1.205
		0.814	1.041
2000	2.971	0.763	1.354
		0.801	1.264
		0.899	1.114

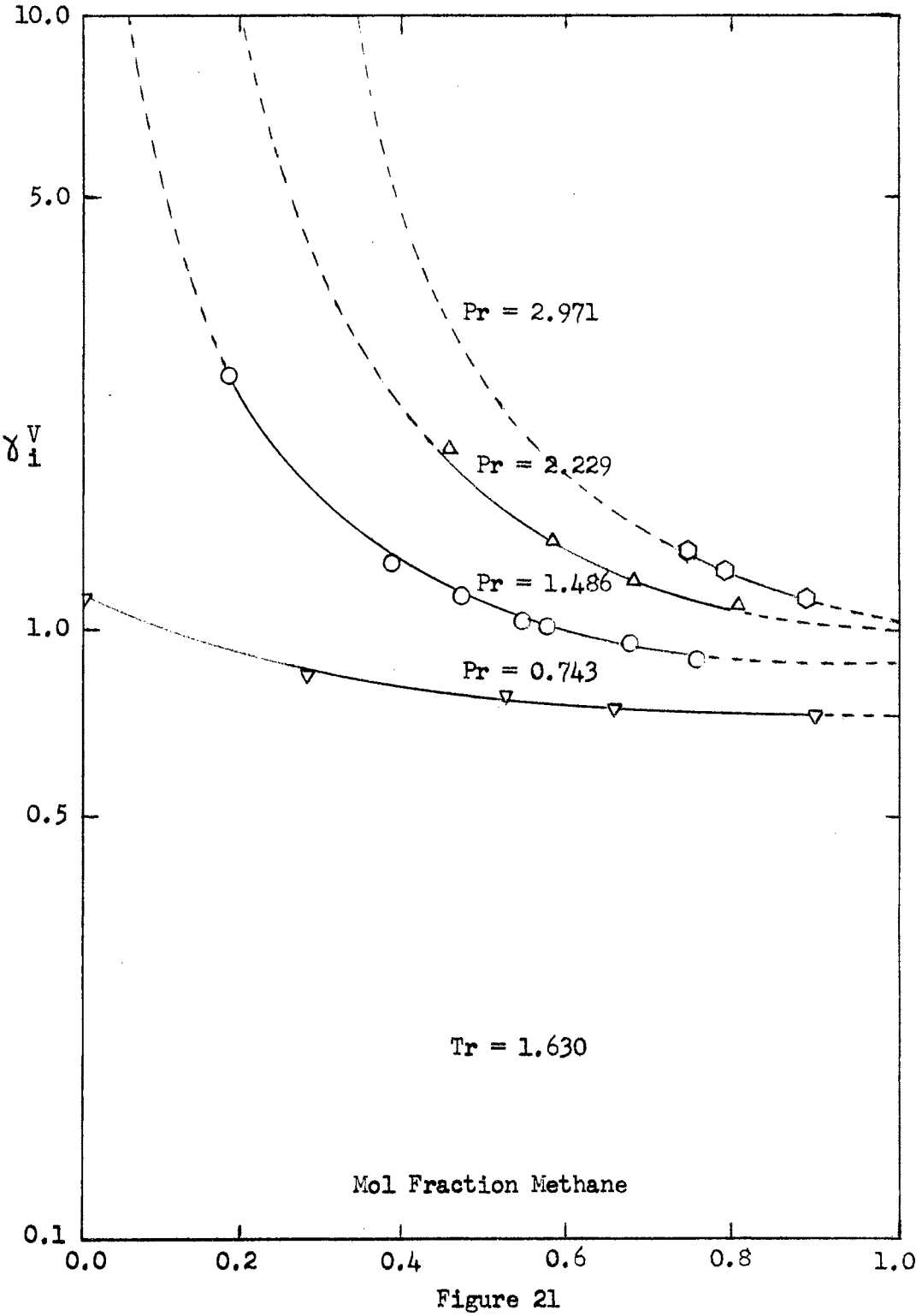

Figure 21

Vapor Phase Activity Coefficient of Methane
in a Methane, Ethane, Normal-Pentane Mixture

Table 11

Data for Figure 22, γ_i^V vs Mol Fraction Ethane in a Methane, Ethane, n-Pentane Mixture

Temperature = 100°F, T_r = 1.018

Pressure Psi	Reduced Pressure	Ethane Vapor-Phase Mol Fraction	Ethane Vapor-Phase Activity Coefficient
500	0.697	0.038	0.326
		0.297	0.324
		0.431	0.328
		0.681	0.326
		0.965	0.329
1000	1.394	0.188	1.025
		0.282	1.017
		0.360	1.004
		0.405	1.001
		0.473	0.994
		0.562	0.978
		0.758	0.914
1500	2.092	0.125	0.831
		0.244	0.815
		0.344	0.773
		0.443	0.683
2000	2.789	0.017	0.681
		0.098	0.641
		0.121	0.627

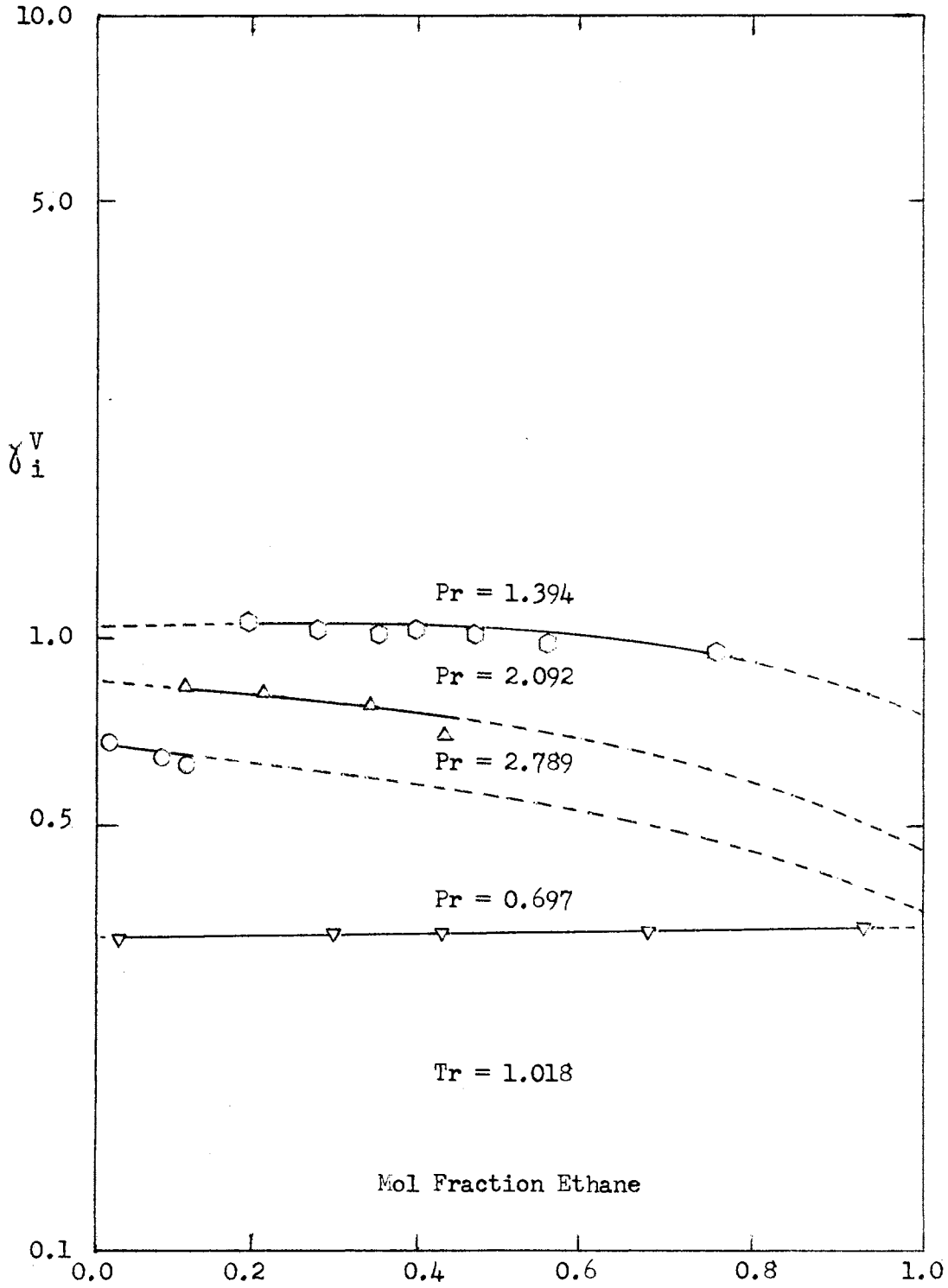

Figure 22

Vapor Phase Activity Coefficient of Ethane
in a Methane, Ethane, Normal-Pentane Mixture

Table 12

Data for Figure 23, γ_i^V, vs Mol Fraction Methane in a Methane, Propane, n-Pentane Mixture

Temperature = 220°F, T_r = 1.980

Pressure Psi	Reduced Pressure	Methane Vapor-Phase Mol Fraction	Methane Vapor-Phase Activity Coefficient
500	0.743	0.059	1.363
		0.170	2.034
		0.329	1.492
		0.345	1.446
		0.571	1.284
1000	1.486	0.397	2.195
		0.521	1.767
		0.566	1.674
		0.669	1.476
		0.714	1.414
1500	2.229	0.542	2.509
		0.598	2.091
		0.689	1.825

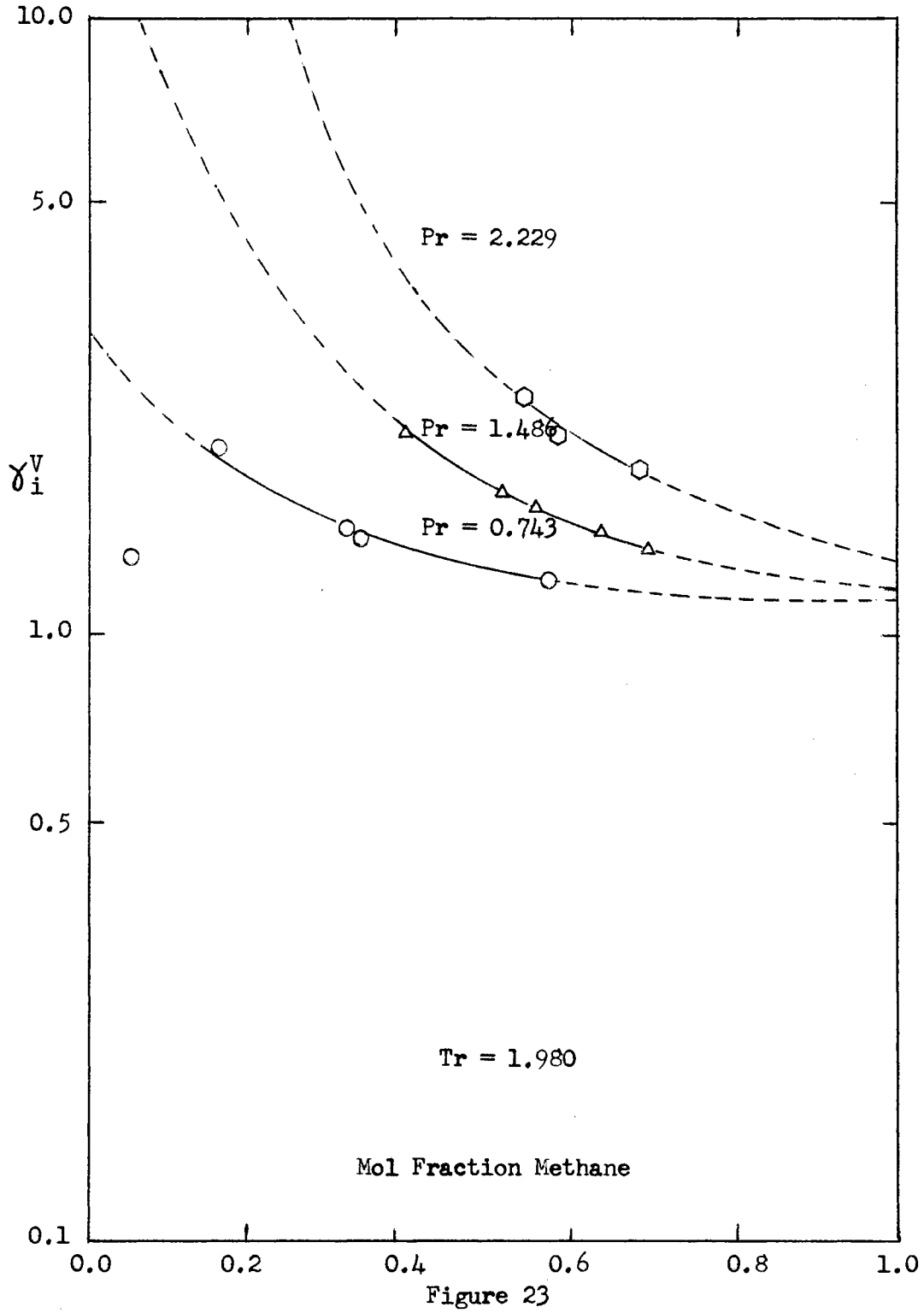

Figure 23

Vapor Phase Activity Coefficient of Methane
in a Methane, Propane, Normal-Pentane Mixture

Table 13

Data for Figure 24, γ_i^V vs Mol Fraction Propane in a Methane, Propane, n-Pentane Mixture

Temperature = 220°F, T_r = 1.021

Pressure Psi	Reduced Pressure	Propane Vapor-Phase Mol Fraction	Methane Vapor-Phase Activity Coefficient
500	0.791	0.190	0.366
		0.451	0.363
		0.472	0.358
		0.666	0.371
		0.809	0.373
1000	1.582	0.106	1.093
		0.155	1.040
		0.264	0.972
		0.318	0.976
		0.463	0.935
1500	2.374	0.108	0.758
		0.194	0.723
		0.239	0.675

CHAPTER VI

CONCLUSIONS AND RECOMMENDATIONS

Conclusions

The Density Integral method of evaluating the imperfection pressure correction term as applied to the ideal K-value is superior to the Pressure Integral method. This is demonstrated particularly in the high pressure region, where for the same number of virial coefficients the Density Integral method gives a much better evaluation.

In the Density Integral method the second and third virials are probably adequate for all subcritical pressure ideal K-value evaluations at, and above, the critical temperature. Additional virial coefficients will be necessary for evaluations at the higher pressures, particularly at the critical temperature where a convergence problem is encountered.

In the Pressure Integral method the second virial is adequate for critical temperature ideal K-value evaluations in the subcritical pressure region, but above this pressure, and for higher temperatures, even the addition of the third virial is not adequate.

The Leiden equation of state expressing compressibility as a function of generalized density seems to be a good basis for deriving virial coefficients, the only drawback being the inaccuracy of the generalized data available. It is definitely a more convenient form

as would be expected. This represents an improvement over the plot shown in Figure 22 where no convergence was obtained. The improvement would apparently be due to the higher reduced temperature. The same errors mentioned in the discussion of Figure 21 would apply, but due to the higher temperature they are not quite so drastic. Figure 24 represents values for propane in the mixture. The reduced temperature in this case was 1.021 and the reduced pressures were 0.791. 1.582 and 2.374. The values obtained corresponded to those in Figure 22 for ethane. in that no tendency to converge was obtained. This case also was for a near-critical temperature.

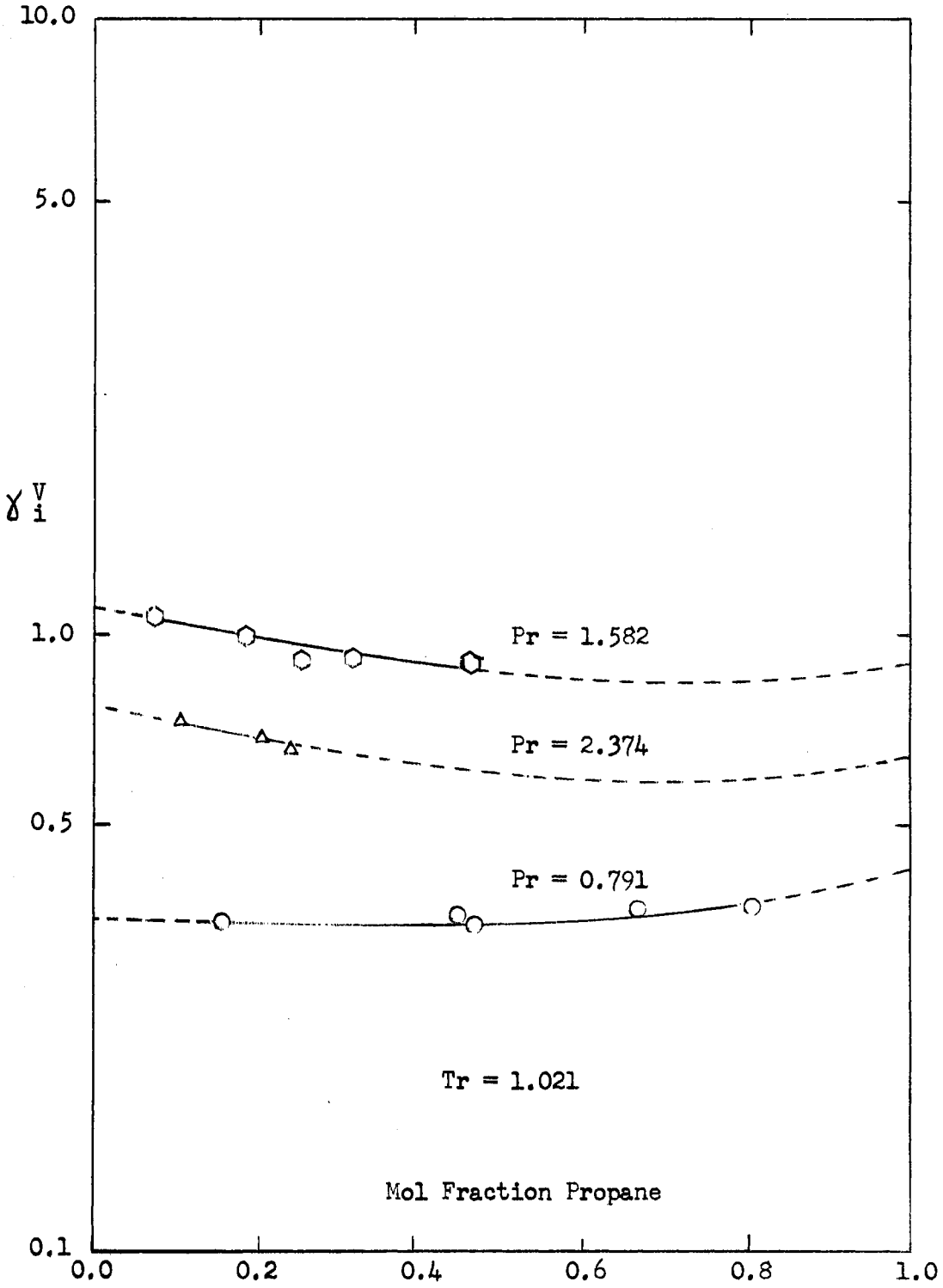

Figure 24

Vapor Phase Activity Coefficient of Propane
in a Methane, Propane, Normal-Pentane Mixture

than a reduced pressure expression.

The second virial coefficient as derived by Pitzer is acceptable in the temperature range from $T_r = 1.0$ to $T_r = 2.0$, but above this it gives values that are too high. Subcritical temperatures were not investigated in this work.

The behavior of ideal K-values at the higher temperatures shows a tendency for a maximum ideal K-value to be reached around $T_r = 3.0$ than for a retrogression to occur.

In the Density Integral method an iterative procedure of interval halving required the most time but gave good results. Newton's method, although faster, gave erroneous results, particularly in the higher pressure region.

Vapor phase activity coefficients can be affected by inaccuracies in ideal K-value evaluation, the reduced vapor pressure evaluation, and the molar liquid volume evaluation. Any one or all of these could be a source of error in the evaluations made. The ideal K-value evaluation could be in error as discussed in the preceding paragraphs. The reduced vapor pressure and molar liquid volume equations could be in need of either a reevaluation of their coefficients, or of more terms.

Recommendations

The Density Integral method is recommended over the Pressure Integral method for use in evaluating the imperfection pressure correction term as applied to ideal K-values.

Values of the generalized Leiden third virial coefficient below the critical temperature should be obtained and a correlation over the entire temperature range ($T_r = 0.8$ to $T_r = 4.0$) be developed as

a function of reduced temperature and acentric factor.

The fourth virial coefficient, at least, should be obtained in order to allow more accurate high pressure evaluation of the imperfection pressure correction term.

Interval halving as an iterative method is recommended for use, Newton's method is definitely not recommended.

Further investigation into the reduced vapor pressure and molal liquid volume evaluations should be considered if the ideal K-value evaluations are revised with no improvement in vapor phase activity coefficient.

BIBLIOGRAPHY

1. Edmister, W. C. Private communication. March, 1963.

2. Edmister, W. C. Private communication. August, 1963.

3. Lewis, G. N. and M. Randall. Thermodynamics, 2nd Edition revised by K. S. Pitzer and L. Brewer, McGraw-Hill Book Co., Inc. (1961).

4. Stuckey, A. N., Jr. "On the Development of an Ideal K-Value Correlation for Hydrocarbons and Associated Gases." (Unpub. M. S. thesis, Oklahoma State University, 1963).

5. Billman, Sage and Lacey. Transactions American Institute of Mining and Metallurgical Engineers, 174, 13 (1948).

6. Dourson, Sage and Lacey. Transactions American Institute of Mining and Metallurgical Engineers, 151, N206 (1943).

7. Scatchard, C. "Equilibria in Non-Electrolyte Solutions in Relation to the Vapor Pressures and Densities of the Components." Chem. Reviews 8, 321 (1931).

APPENDIX A

NOMENCLATURE

b - generalized Leiden second virial coefficient

B - Leiden second virial coefficient

B' - Berlin second virial coefficient

B'' - generalized Berlin second virial coefficient

c - generalized Leiden third virial coefficient

C - Leiden third virial coefficient

C' - Berlin third virial coefficient

C'' - generalized Berlin third virial coefficient

f^L - liquid phase fugacity

f^V - vapor phase fugacity

K - vapor-liquid equilibrium constant

K_I - ideal vapor-liquid equilibrium constant

K_I^o - simple fluid ideal vapor-liquid equilibrium constant

K_I' - deviation from simple fluid ideal vapor-liquid equilibrium constant

p^o - vapor pressure

P - system pressure

Pc - critical pressure

Pr - reduced pressure

R - universal gas constant

T - temperature

T_c - critical temperature

T_r - reduced temperature

V^L - molar liquid volume

V - molar vapor volume

x - mole fraction in the liquid phase

ρ_r - reduced density

y - mole fraction in the vapor phase

Z - compressibility factor

Z^o - simple fluid compressibility factor

Z' - deviation from simple fluid compressibility factor

Z_{Pr} - compressibility at reduced system pressure

$Z_{p_r^o}$ - compressibility at reduced vapor pressure

γ^L - liquid phase activity coefficient

γ^V - vapor phase activity coefficient

θ - imperfection pressure correction term

ω - acentric factor

δ - solubility parameter

i - subscript indicates value is for a particular component

APPENDIX B

EQUATIONS

The equation for reduced liquid volume is (4)

$$\frac{V_i^L P_c}{RT_c} = (0.03161 - 0.00436\omega)(5.7 + 3T_r) \qquad \text{(B-1)}$$

The equation for reduced vapor pressure is (4)

$$p_r^o = 5.1788022 - \frac{5.1331403}{T_r} - \frac{0.0456619}{T_r^2} \qquad \text{(B-2)}$$

The Scatchard-Hildebrand liquid phase activity coefficient is obtained from the equation (7)

$$\ln \gamma_i^L = \frac{V_i^L}{RT} (\delta_i - \bar{\delta})^2 \qquad \text{(B-3)}$$

Where: V_i^L is obtained from Equation (B-1)

δ_i is the component solubility parameter

$$\bar{\delta} = \sum x_{V_i} \delta_i \qquad \text{(B-4a)}$$

$$x_{V_i} = \frac{V_i^L x_i}{\sum V_i^L x_i} \qquad \text{(B-4b)}$$

VITA

James Ralph Randall

Candidate for the Degree of

Master of Science

Thesis: IMPERFECTION PRESSURE CORRECTIONS FOR PREDICTION OF IDEAL VAPOR-LIQUID EQUILIBRIUM RATIOS

Major Field: Chemical Engineering

Biographical:

Personal Data: Born in Tulsa, Oklahoma, December 5, 1933, son of Herman R. and Hattie E. Kelton. Married to Jean Summers, Gore, Oklahoma, in June, 1955. Son Martin, daughters Lorena and Jana.

Education:

Attended elementary schools in Sallisaw, Agra, Claremore and Tulsa, Oklahoma; graduated from Will Rogers High School, Tulsa, Oklahoma in 1951; majored in Forestry and Chemical Engineering at Oklahoma State University and The University of Tulsa; received the Bachelor of Science degree in Chemical Engineering from Oklahoma State University in May, 1957; received certificate of completion in Meteorology from Oklahoma State University in August, 1958, while in the Air Force; completed requirements for Master of Science degree in May, 1965.

Professional Experience:

Employed as a Junior Engineer with Sunray Mid-Continent Oil Company, Tulsa, Oklahoma in summer of 1956. Employed as a Process Engineer with International Paper Company, Springhill, Louisiana from June, 1957 to August, 1957. Employed as a Production Superintendent with Crosby Chemicals, Inc., Picayune, Mississippi from March, 1960 to May, 1962. Presently employed as an Engineer with Cities Service Oil Company, Tulsa, Oklahoma.